A FUNDAMENTAL STUDY OF MAGNETIZING PROCESS IN HOMOGENEOUS SEDIMENTS BY THEORETICAL AND OBSERVATIONAL APPROACH

兵頭，政幸

(Degree)
博士（学術）
(Date of Degree)
1985-03-18
(Date of Publication)
2007-10-16
(Resource Type)
doctoral thesis
(Report Number)
乙0966
(URL)
https://hdl.handle.net/20.500.14094/D2000966

神戸大学博士論文

A FUNDAMENTAL STUDY OF MAGNETIZING PROCESS IN HOMOGENEOUS SEDIMENTS BY THEORETICAL AND OBSERVATIONAL APPROACH

（堆積物の磁化機構に関する理論と実験観測による研究）

CONTENTS

AKNOWLEDGEMENT

The auther wishes to express his cordial thanks to Professor K. Yaskawa for his instructive advice and encouragement throughout this study. He is indebted to Associate Professor N. Isezaki for his helpful suggestions and discussions.

Thanks are due to Professor F. Arai of Gunma University for his critical comments on the tephrochronological ages in lacustrine deposits by analysing the volcanic ash, to Professor A. Yamamoto of Osaka Electro-Communication University for the permition to quote his results in advance of publication, to Dr. Maeda of Kobe City Institute for Educational Research for his helpful advice on tephrochronology and to Professor M. Ozima of the University of Tokyo for many stimulating discussions and encouradgement.

The author is grateful to Drs. J. Matsuda and Y. Otofuji for many valuable suggestions and discussions. He also expresses his appreciation to many colleagues of Marine Geophysics Laboratory, Kobe University for a lot of helpful discussions and to Miss S. Onishi for her kind help in preparing the manuscript.

ABSTRACT

Magnetization process of a sediment is formulated using a linear system theory. Remanent magnetization is represented as a convolution integral of a geomagnetic field variation and a moment fixing function. The formulated model predicts that magnetization of sediments records a field variation deformed through a filter, and that the original field can be deduced from the record of magnetization by a deconvolution method.

Applying the linear system model to the magnetization data of seven core-sediments from central to south-western Japan, a method to assess quality of magnetization record in a core is developed, and then a reliable variation curve of the geomagnetic field direction for the last 11000 years is deduced. Moreover, it is demonstrated that the remanent intensity change is reflected by the intensity reduction due to cancellation of anti-parallel magnetic moments resulted from the integration of field variation not only during polarity transition but also in the same polarity period.

The general motion of the non-dipole source for the last 7000 years expected by the secular variation in south-western Japan shows both westward and eastward drifts, whose periods are all about 500 to 1000 years. The two drifts alternatively occur for the last 3000 years and the westward drift prevails in the period from 7000 to 5500 years B.P..

PART I - THEORY

1. Introduction

Magnetic study of rocks has greatly contributed to elucidate the history and the nature of geomagnetism. One of the most important contributions was the discovery of repeated changes in polarity of the earth's magnetic field (Matuyama, 1929 ; Cox et al., 1963, 1964). These works were followed and developed by many investigations based on measurements of the magnetization with the radio-isotope age of igneous rocks. During the last decade the geomagnetic stratigraphy thus obtained, being slightly modified, was confirmed through analysis of the geomagnetic anomaly observed on/over the ocean surface and by the fact that the core sediments from the ocean bottom have the sequence of normal and reversed remanence.

Knowing the stable remanence of ocean bottom sediments led us to try to trace back more detailed behaviors of the geomagnetic field in the past with unconsolidated sediments rapidly deposited in the lake. Then a number of events and excursions of different ages were discovered in many places (Clark & Kennett, 1973 ; Yaskawa et al, 1973 ; Denham, 1974). It is an advantage that the chronological continuity in sediment samples enable us to trace back movement of the geomagnetic field direction without interruption. In recent years the paleomagnetism using sediments is extended to an investigation of the geomagnetic secular variation in the Holocene time (Creer et al., 1972 ; Creer et al., 1976 ; Hyodo & Yaskawa, 1980 ; Hyodo et al., 1984 ; Hyodo & Yaskawa ,1984a ; Hyodo & Yaskawa , 1984b ; Hyodo & Yaskawa, 1984c). Such a study on a secular variation requires much higher precision and resolution in records of the geomagnetic field than that on polarity changes alone. However, detailed features of remanent magnetization of sediments are not clarified sufficiently enough to meet the requirement of geophysicists engaged in research on the geomagnetism, especially on its secular variations.

Irving (1957) has discussed using the post depositional detrital remanent magnetization (PDRM) model that the magnetization of natural sediments is acquired accurately in alignment with a direction of an ambient field without any inclination error. The model was confirmed experimentally with both synthetic and natural sediments (Irving & Major, 1963; Kent, 1973). We also have some observed data from lake sediments which support the PDRM model. Two cores of sediment from lake St. Croix have the same magnetic records of high degree of correspondence in the magnetization directions (Lund et al, 1976). Similar curves of directional changes in remanence have been observed in many cores from several lakes in Britain (Turner & Thompson, 1981), although they show somewhat lower degrees of correspondence than that of lake St. Croix. Moreover, the observed paleo-inclinations are close to the values calculated at the site with a central dipole field. These facts appear to suggest that sediments acquire remanent magmetization being at least controled by the geomagnetic field, and the same change of magnetization can be observed in different core-sediments even from distict basins when they meet some conditions.

We cannot easily conclude that a PDRM points to the true direction of a past geomagnetic field even if several sediment columns bear the same records of changes in remanent magnetization. Each record may have undergone the same deformation to deviate from the true field direction. Another question is that there has been no observation of the same records of magnetization in sediments whose past depositional environments differ largely, in particular, accumulation rates are extremely different. The author formulates the magnetizing process in a continuous sediment column, and discusses a geomagnetic secular variation to be recorded in the remanence being deformed and a possibility to reconstruct the original secular variation from the magnetization record.

2. A linear system model

2.1 Description of PDRM

A general concept of PDRM is as follows. Magnetic grains in a sediment are free to rotate in the water-filled voids of matrices even after deposition and are aligned along the external magnetic field. As the voids are gradually reduced by the weight of the overlying sedimentary column, the grains become hard to move and eventually cease to rotate, leaving the magnetization directions parallel to the ambient field. The fixing of a magnetic grain is attained by a balance of two opposing forces ; a magnetic torque and a mechanical resistance. The magnetic torque is expressed by a vector product of the magnetic moment of the particle and the external field. The mechanical resistance is caused by viscosity of the surrounding fluid and a friction with void wall. The particle is fixed when the resistant force predominates the magnetic torque.

Experimental tests have been attempted by many investigators. They can be classified into three types. (a) A long column of sediment is formed grain-by-grain deposited during a long term (Løvlie, 1974, 1976 ; Barton & McElhiny, 1979). (b) A slurry is poured into a container or a short column. The PDRM component was measured at various depths in a short column (Tucker, 1980). The degree of compaction was replaced with water content of a sample (Payne & Verosub, 1982). (c) A specimen is compressed using an apparatus (Hamano, 1980 ; Otofuji & Sasajima, 1981). A sediment was compacted with various degrees which correspond to depths in a natural sediment. Partial magnetization acquired over some degree of compaction was measured.

Three characteristic features of depositional detrital remanent magnetization (DRM) have been revealed from many experimental results. The first is that most of the remanences of sediments are ascribed to PDRM components. Second, in a uniform field the magnetization to be acquired in each depth decreases as depth goes down. Hamano (1980) discussed on a red clay that magnetization acquisition starts from the depth of 15 cm, half of the total remanence being acquired at 80 cm depth, and is completed at 2.5 m. The third is that the partial PDRM acquired in some compaction range has an additive property (Otofuji & Sasajima, 1981). If a partial magnetization acquired in a uniform field over the depth range from d_0 to d_1 ($d_0 < d_1$) is denoted by $M_{d_0}^{d_1}$, partial magnetizations $M_{d_0}^{d_1}$, $M_{d_1}^{d_2}$ and $M_{d_0}^{d_2}$ have the following relation;

$$M_{d_0}^{d_2} = M_{d_0}^{d_1} + M_{d_1}^{d_2} \quad (d_0<d_1<d_2)$$

This law was realized even when the field direction was reversed or the field strength was changed during the compaction process. This fact leads to a possibility that the magnetization of sediment can be represented by a supperposition of components acquired in different ages.

2.2 Formulation of a magnetizing process

Let us consider a thin sediment sheet produced for unit time width in a long core with unit cross section. It contains magnetic grains of various sizes with different intensities. The sediment sheet is subjected to gradual compaction after deposition and then the void volume formed by relatively large grains, in which smaller magnetic particles can rotate to align along the ambient field, is reduced with time. The following increases in viscosity of fluid and in friction with void wall cause blocking of magnetic particles. The magnetic particles do not cease to rotate simultaneously, but they are partially fixed in various stages of different degrees of compaction. The resultant magnetization of the sediment is the sum of the magnetic moments of particles gradually fixed.

To express the change of the partial fixing quantitatively, we define a function r(t) ; the amount of magnetic moment blocked at t in a unit sediment sheet. The r(t) appears to be able to be expressed by an exponential function, approximating the experimental result that magnetizing starts from a depth 15 cm, a half of a total remanence is acquired at a depth 80 cm and it is completed at a depth 250 cm. The function was given as in Eq.1.

$$r(t) = C\, e^{-At} \quad (1)$$

$$r(t) = 0 \quad (t < t_0) \quad (1.1)$$

$$\int_{t_0}^{\infty} r(t)\, dt = 1 \quad (1.2)$$

$$\int_{t_1}^{\infty} r(t)\, dt = 0.5 \quad (1.3)$$

$$\int_{t_2}^{\infty} r(t)\, dt = 0 \quad (1.4)$$

where coefficients A and C are constants, t_0, t_1 and t_2 ($t_0<t_1<t_2$) represent times of onset of magnetization, completion in the fixing of a half magnetic moments and end of the moment fixing. The integral value of r(t) is normalized by m_0, amount of the total magnetic moment to be fixed in a uniform field of intensity

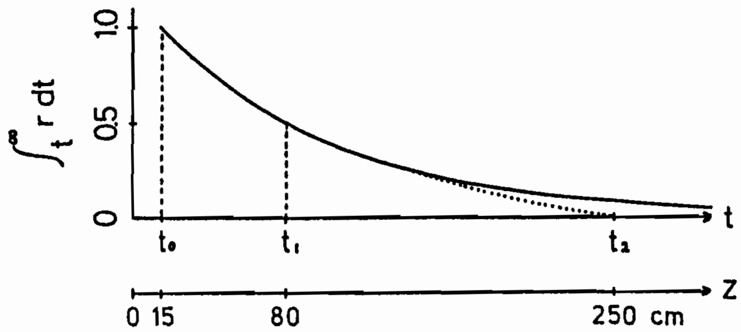

Fig.1 Moment fixing function r(t). The solid line shows an exponential curve. The dotted line shows a curve from experiment.

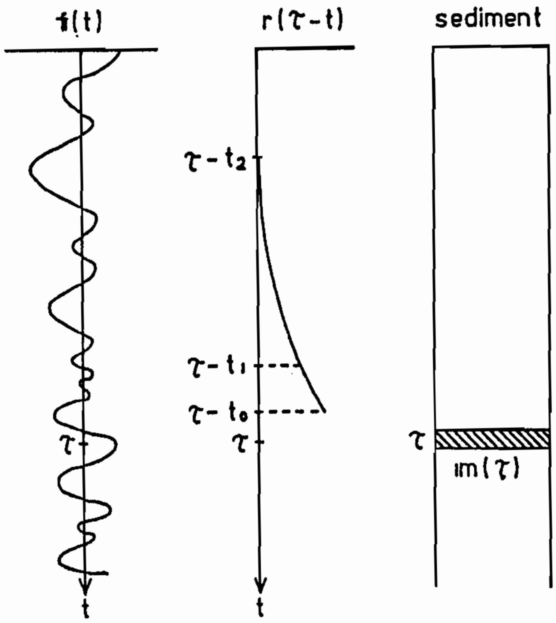

Fig.2 A schematic view of the present model. The shaded area shows a unit sediment sheet of age τ, whose magnetization is shown by **m**(τ). The **f**(t) shows a secular variation of geomagnetic field vector. The r(τ-t) represents a moment fixing function for the unit sediment.

f_0. Eq.1 is illustrated in Fig.1 being integrated. The solid line shows the integrated r(t) of the exponential function and the dotted line represents that of the one based on the experimental result. A difference between them is that the latter has an end point of fixing at t_2. There is a small discrepancy below 1.5 m between the two curves. However, its contribution to the total remanence is expected small.

Assuming that the axis of magnetic moment fixed at t is aligned in parallel with the geomagnetic field and each moment is additive, the magnetization of a unit sediment sheet of age τ, which has been exposed to a geomagnetic field variation $\mathbf{f}(t)$ from τ years ago through to present, can be expressed as follows:

$$\mathbf{m}(\tau) = \int_0^\tau \frac{m_0}{f_0} \mathbf{f}(t)\ r(\tau - t)\ dt \qquad (2)$$

$$(t_2 < \tau)$$

where $\mathbf{m}(\tau)$ is the magnetization and t shows the age axis which has its origin in the sediment/water interface and increases downward. We must note that the t in Eq.2 differs with that in Eq.1, the time after deposition. The schematic view of Eq.2 is illustrated in Fig.2. The curve of $\mathbf{f}(t)$ on the left shows the geomagnetic field vector corresponds to the age of each horizon in the sediment column. Since the unit sediment sheet of age τ, expressed by a shaded portion in Fig.2, acquires remanent magnetization through a duration from t_0 to t_2 after deposition, namely, from $t = \tau - t_0$ to $t = \tau - t_2$, the moment fixing function r(t) is given as drawn in Fig.2.

This formula implies that the magnetization of a sediment can be calculated by a convolution integral of a magnetic field variation $\mathbf{f}(t)$ and a moment fixing function r(t). In addition, it suggests two important features of magnetization. One is that the direction of magnetization does not coincide with that of the external field unless $\mathbf{f}(t)$ is constant in direction or the $r(t)$ is the Dirac's δ function. The other is that the magnetization intensity is shown by a product of the component proportional to the field intensity and the component of intensity reduction caused by the cancellation due to the superposition of magnetic moments aligned in various directions. The latter component results from the integral of the directional change of field.

2.3 Effect of moment fixing function r(t)

Considering the four associated conditions of Eq.1, the integral limits of Eq.2 can be extented as:

$$\mathbf{m}(\tau) = \int_{-\infty}^{\infty} \mathbf{fe}(t)\ r(\tau-t)\ dt \qquad (3)$$

where $\mathbf{fe}(t) = (m_0/f_0)\mathbf{f}(t)$. Since Eq.3 is a convolution integral, it can be described by spectra using the Fourier transform as:

$$\mathbf{M}(\omega) = \mathbf{Fe}(\omega)\ R(\omega) \qquad (4)$$

where $\mathbf{M}(\omega)$, $\mathbf{Fe}(\omega)$ and $R(\omega)$ are spectra of $\mathbf{m}(t)$, $\mathbf{fe}(t)$ and $r(t)$, respectively. Eq.4 shows that the spectrum of magnetization $\mathbf{M}(\omega)$ can easily be calculated only by multiplying $\mathbf{Fe}(\omega)$ by $R(\omega)$, whereas in the space domain the magnetization $\mathbf{m}(t)$ is obtained by filtering $\mathbf{fe}(t)$ with a filter $r(t)$. The $R(\omega)$ provides us detailed properties of the filter.

If we put $t_0 = 0$ since $t_0 \ll t_2$, Eq.1 becomes as:

$$r(t) = A\ e^{-At} \qquad (A = \ln 0.5/T_{1/2}) \qquad (5)$$

where $T_{1/2}$ is a period for the fixing of a half magnetic moments.

Thus the moment fixing function r(t) can be determined by only $T_{1/2}$, i.e. only the condition (1.3) is enough for the determination of r(t).

Since r(t) = 0 when t<0, the Fourier transform of r(t) becomes as:

$$R(\omega) = 1 / (1 + (\omega/A) i) \qquad (6)$$

To examine the properties of $R(\omega)$ in detail, we separate it into real part and imaginary part, which show an amplification and a phase lag, respectively. The amplitude spectrum becomes as:

$$|R| = 1/\sqrt{1 + (\alpha T_{1/2}/T)} \qquad (7)$$

$$(\alpha = 2\pi/\ln 0.5)$$

and the phase spectrum becomes as:

$$\theta = \tan^{-1}(\alpha T_{1/2}/T) \qquad (8)$$

where $T = 2\pi/\omega$. Eq. 7 and 8 show that both spectra are functions with respect to $(T_{1/2}/T)$, the ratio of the half fixing period to the wavelength of the field variation. The properties of the filter are illustrated in Fig.3. We also simulated the effect of the filter from experimental result shown by a dotted line in Fig.1 which has a terminal point of magnetizing. Both amplification and phase lag of the filter show almost the same change to those of the exponential one, although small fluctuations occur in the curve of phase lag. If we adopt a linear function instead of an exponential, a more pronounced fluctuation, whose frequency is determined by the width of moment fixing zone, will emerge in both amplification and phase lag. Anyway the use of an exponential is appropriate for the approximation of the moment fixing function.

According to secular variations of geomagnetic field from

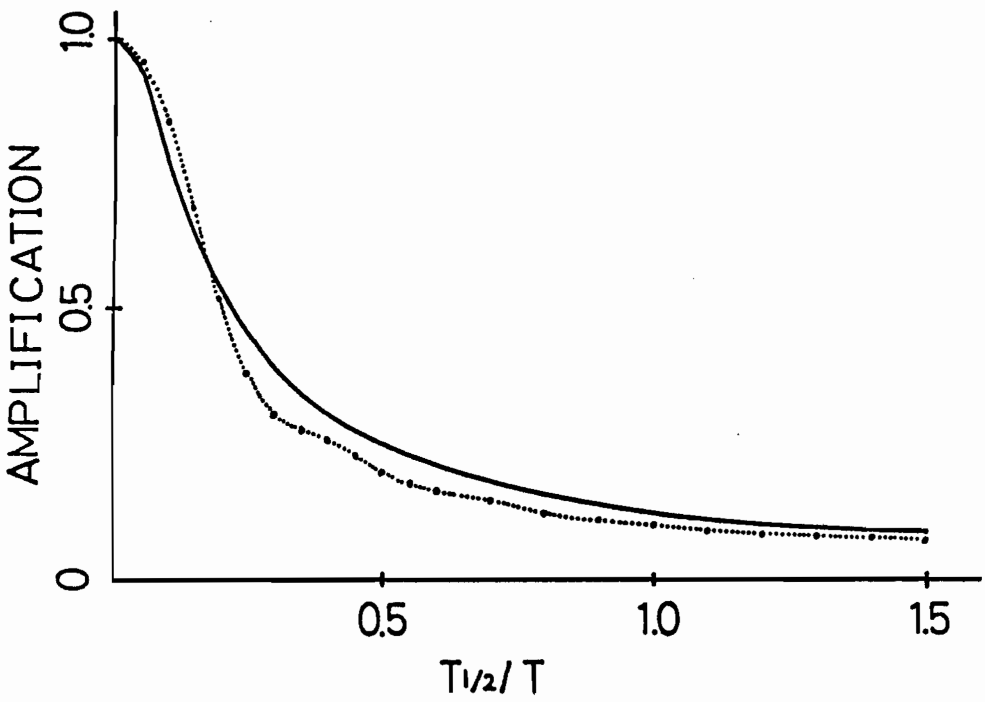

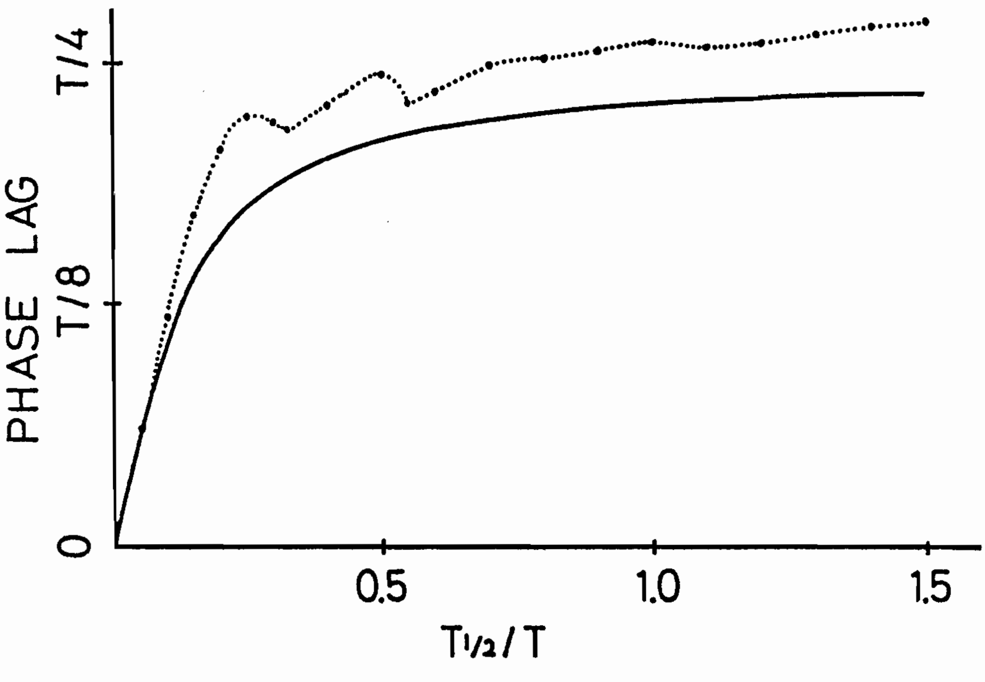

Fig.3 Amplification and phase lag by the filter R. The solid lines are based on Eq.7 and 8. The dotted lines are simulated ones using a function from experiment.

archeomagnetism (Hirooka, 1971; Kovacheva, 1980), there is no directional offset over 20° from a mean direction. Therefore, we can regard the change of declination and inclination approximately linear to the orthogonal axis, and the amplitude attenuation and the phase lag shown in Fig. 3 are applicable to the deformation of declination and inclination curves. As shown in Fig. 3, a large ($T_{1/2}/T$) give rise to a large amplitude attenuation and a large phase lag in declination and inclination. If the $T_{1/2}$ is kept constant, the components of higher frequency are more deformed. On the other hand, a large $T_{1/2}$, which is equivalent to a small depositional rate, causes a large deformation. For instance when $T_{1/2}$= 500 yr, the directional change of T = 500 yr is deduced to 0.13 and its phase is delayed by 115 yr and that of T = 250 yr to 0.25 and by 53 yr. Thus a secular variation of the earth's field is deformed variously by different filters.

3. Half fixing depth of deep-sea sediments

If the above model is considered on depth axis instead of time, half fixing depth $Z_{1/2}$ should be defined in place of half fixing time $T_{1/2}$. The $Z_{1/2}$ can be used as a parameter expresses width of remanence acquisition zone. We try to estimate the half fixing depth $Z_{1/2}$ for natural sediments. A clear value for $Z_{1/2}$ can be calculated with the remanent intensity of deep sea sediments. It shows a progressive decrease prior to a polarity transition and an immediate recovery after that. The intensity drop shows a convex decrease and the following recovery a concave increase. These features are not only observed in natural deep-sea sediments (Opdyke et al., 1966; Harison & Somayajulu, 1966; Kobayashi et al., 1971) but also explained by some models (Iøvlie, 1976; Niitsuma, 1977; Otofuji & Sasajima, 1981).

The present model is applied to the magnetization data of the core KH 68-4-20 (Kobayashi et al., 1971). The remanent intensities and polarities determined from directions of remanence are shown in Fig.4(a). Intermediate directions of magnetization are not observed at the positions of polarity transition. Four successive polarity changes occur during the depth from 3.52 m to 5.50 m. The two reversals at 3.52-4.10 m and 4.75-5.50 m are paleontologically interpreted as the Kaena and the Mammoth events. Their ages determined from volcanic rocks (Labrecque et al, 1977) are shown in Fig.4(b). The intensity drop at the reversals, caused by only the cancellation of magnetic moments aligned in the opposite directions, was calculated using Eq.2 with a field expressed by the polarity

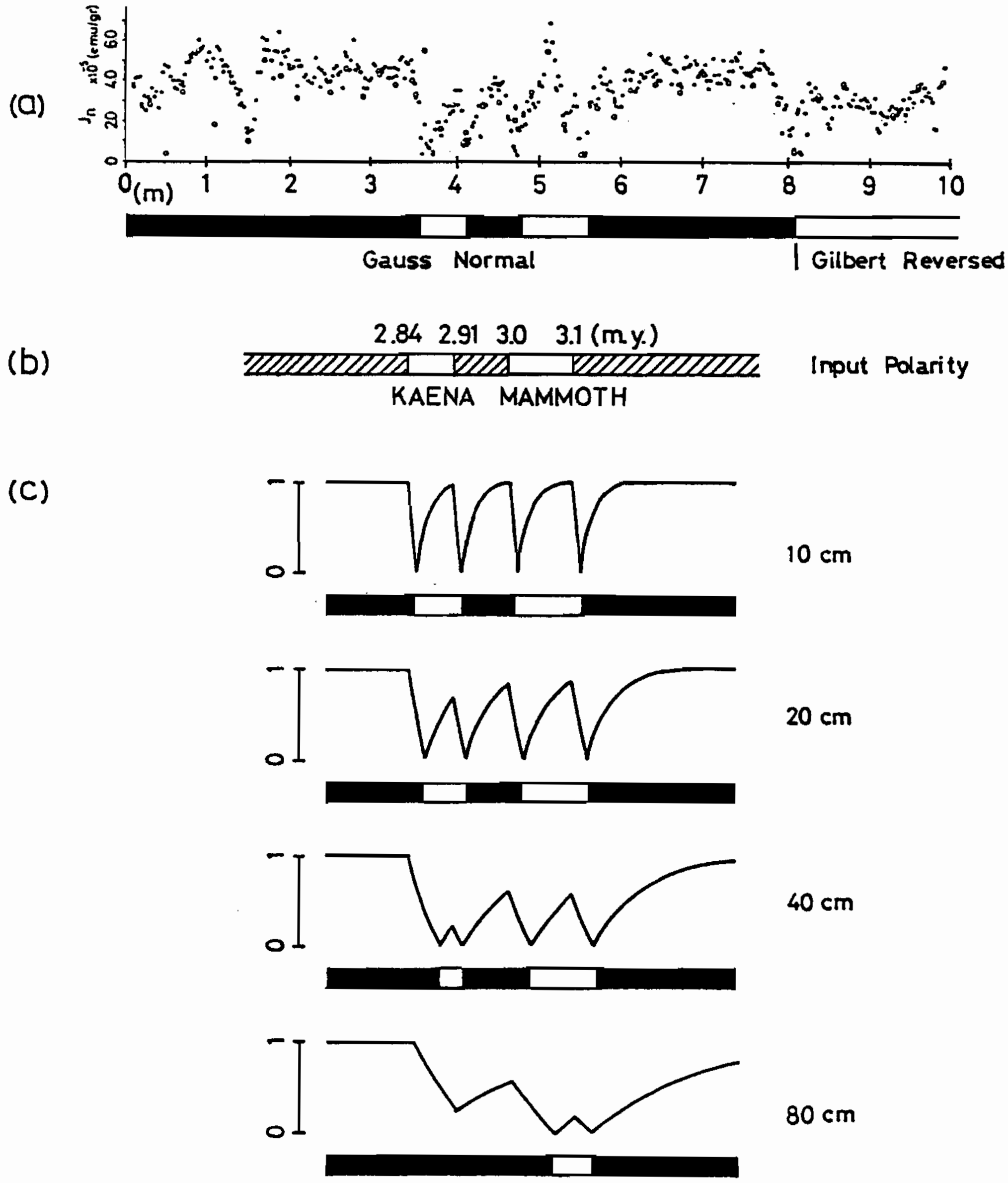

Fig.4 Intensity reduction due to cancellation in the polarity transition zone. (a) Magnetization intensities of deep sea sediment of the core KH-68-4-20 (after Kobayashi et al., 1971). (b) Polarity change of the input field. (c) Intensity patterns calculated with a field of the polarity change shown in (b). The right figure represents $Z_{1/2}$ used in the calculation of each curve.

change in Fig.4(b) assuming that the depositional rate is constant at 7.6 mm/10^3yr. The calculations were carried out using four kinds of moment fixing function with $Z_{1/2}$= 10, 20, 40, and 80 cm (Fig.4.c). The results shown in Fig.4(c) represent that the shape of intensity pattern considerably changes with $Z_{1/2}$. The uppermost intensity peak in the three successive ones diminishes as $Z_{1/2}$ becomes large. The peak disappears completely when $Z_{1/2}$ reaches the width of the Kaena event. Then positions of polarity boundary are shifted downward with increasing $Z_{1/2}$. The result of calculations reveals that a polarity transition is shifted downward by $Z_{1/2}$ and a small event shorter than $Z_{1/2}$ is not recorded in magnetization direction, although the trace is still remained in intensity. The intensity pattern calculated with $Z_{1/2}$ of 20 cm seems to fit best the observed one. Thus the remanent intensity drop during a reversal can be explained by only the cancellation effect on the assumption that the field intensity is constant.

According to some studies with volcanic rocks and intrusions, the intensity of the earth's field is decreased at a polarity transision. However, we can not know if the duration of the field intensity decrease is as long as those recorded in sediments, since the studies on polarity transition zone with igneous rocks can not be made on time axis.

Width of a remanent intensity drop at a single reversal in sediments is usually less than 50 cm. No matter how fast a sediment is accumulated, the drop width in the sediment does not extend beyond this value. This fact suggests that the remanent intensity drop during a reversal in sediments is independent on the field intensity. If the intensity change consists of only the cancellation effect, a quite small $Z_{1/2}$ is enough to produce the intensity drop. Even the moment fixing function whose $Z_{1/2}$ is only 12 cm can produce the intensity drop more than 10 % over the width 30 cm. Many drops which extend over 10 cm or less were observed in densely measured cores of deep sea sediments (Sato, 1980). To make out an intensity drop of 10 cm-width, 2.5 cm is enough for the half fixing depth. Thus the small value 10 cm or less is generally appropriate for $Z_{1/2}$ of deep sea sediments.

4. Possibility to obtain a secualr variation

Let us consider a possibility to obtain a secular variation of geomagnetic field from sediments. The effect of the filter r(t) is described with depth axis in Fig.5. Amplification and phase lag of a secular variation of the earth's field, whose wavelength is expressed in centi-meter, are shown on several half fixing depths. When $Z_{1/2}$ is 40 cm, significant attenuation in amplitude and phase lag occur throughout the wavelength range from 0 to 400 cm, their grade depending on the wavelength. Therefore, such a sediment does not preserve accurate paleo-field directions. On the other hand, when $Z_{1/2}$ is 5 cm, the deformation due to the filter becomes small ; on the components of wavelength over 50 cm, the decrease in amplitude is less than 20 % and phase lag is only 4 to 6 cm, both curves of which are flat throughout the wavelength range more than 100 cm. The geomagnetic field direction appears to be recorded faithfully in a sediment of small $Z_{1/2}$. However, when we discuss the components of high-frequency less than 50 cm in wavelength, we should take the effect of the filter into consideration. If a sediment column has a constant $Z_{1/2}$ throughout the length no matter how large the $Z_{1/2}$ is, a secular variation can be deduced from its magnetization record using the convolution method.

On the remanence preserved in sediments of large $Z_{1/2}$, some problems can be inferred. When a secular variation of the geomagnetic field is recorded in sediment columns of different depositional rates, the recorded signals not only have different wavelengths but also undergo different filterings. These

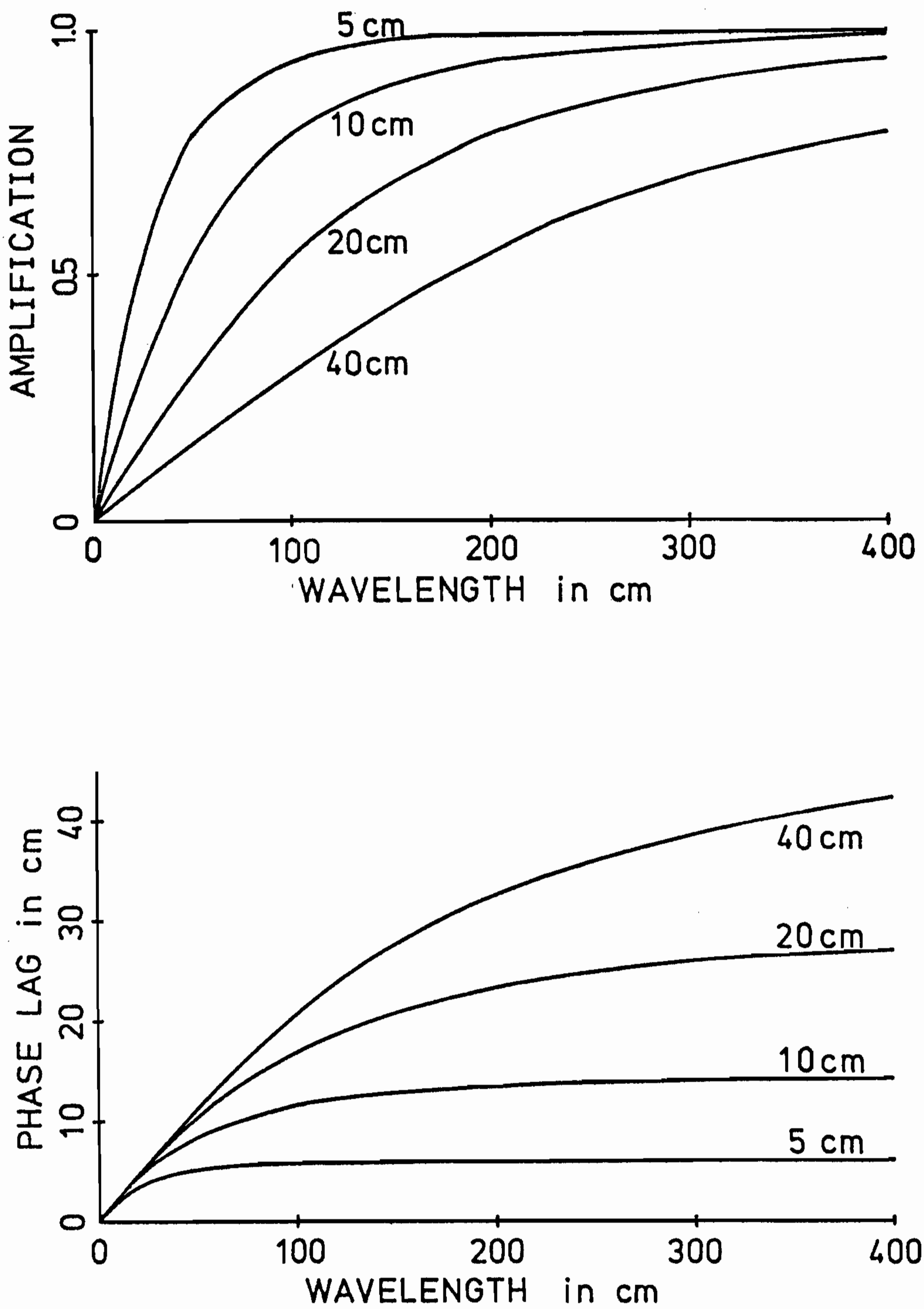

Fig.5 Amplification and phase lag due to the filter R of $Z_{1/2}$ = 5, 10, 20 and 40 cm.

sediments have distinct variations of magnetization, even if their half fixing depths are the same. This matter may cause that no good-coincidence exists in secular variation curves of the earth's field from various sediment columns with quite different depositional rates. In addition, change curves of declination and inclination, whose wavelengths of main spectra are extremely different with each other, are recorded with some difference in their phase lags. This matter provides us some warning in using the declination and inclination curves of remanence in sediments as a time scale. When depositional rates or half fixing depths vary with depth in a sediment column, it is quite difficult to reconstruct the original field variation from the magnetization of the sediment.

In addition to the deformation of declination and inclination curves, the model shows the existence of an important feature in remanent intensity. It is that there is an intensity change due to decrease by cancellation of magnetic moments aligned in various directions. Intensity pattern during geomagnetic reversals, often observed in deep-sea sediments, was finely explained by only the component due to cancellation. The cancellation occurs even in a period with the same polarity. Intensity of magnetization of sediment is a resultant of a component proportional to field intensity and a component due to the cancellation. It is required to separate the two components to obtain a secular variation of field intensity.

PART II - OBSERVATION

5. Introduction

Paleomagnetic studies with young sediments after pleistocene have increased in number since a pioneer work was done in Lake Windermere, Englang (Mackereth, 1971). In Japan, these investigations were started with lacustrine deposits in Lake Biwa (Yaskawa et al., 1973) and followed in Lake Kizaki (Horie et al., 1980). In recent years, many paleomagnetic works on the Holocene sediments have been made, using giant core samples from middle to south-western Japan (Hyodo & Yaskawa, 1980 ; Hyodo et al., 1984 ; Hyodo & Yaskawa, 1984a ; Hyodo & Yaskawa, 1984b ; Hyodo & Yaskawa, 1984c). The sediment samples have undergone different depositional environments and they are composed with distinct materials. Therefore these sediments will provides us a lot of information on remanent magnetization of various sediments to approach the intrinsic mechanism of magnetizing. We examine several features of PDRM expected from the present model to assess the reliability of the model and then assess the quality of the magnetization records in individual cores. Moreover, we eventually deduce a secular variation of the geomagnetic field in this area, which is the main purpose of these works.

6. Sampling and measurement

Sampling was made with a giant piston core sampler, whose core pipe is 20 cm in diameter and 10 m in length. It is assembled by connecting stainless pipes 1 m long, and therefore it can be extended as long as it is needed. It attaches a 500 kg hammer on the head to enable the pipe penetrate through sediment by percussion even after the penetration by gravity is stopped by friction. A long horizontal arm is stretched on the top to prevent from rotation at coring. The whole view of the corer is shown in Fig.6. The sediment sample raised is divided into 1 m segments by separating the core pipes with sediment included. Preparation of specimens of 1 inch size for measurement were made by two methods as shown in Fig.6. There was no difference between the two methods in quality of magnetization data.

A total of 7 core samples of sediment have been collected from the Inland Sea, Japan (Seto Naikai) and two lakes in central Japan : five cores of shallow water sediments are from Osaka Bay (cores OS1, OS2 and OS3), Harima-nada (core HR1) and Mizushima-nada (core MZ1), and two cores of lacustrine deposits from Lake Yogo (core YG1) and Lake Kizaki (core KZ3). The coring sites are shown in Fig.7. Most of the cores of shallow water sediment consist of uniform material of clay or silt throughout lengths without any laminae. This fact indicates that the sediments have been deposited in uniform environment after the Holocene transgression. In the core MZ1, however, there is a distinct unconformity at 50 cm from base, at which material suddenly changes from coarse sand to fine clay. It has been

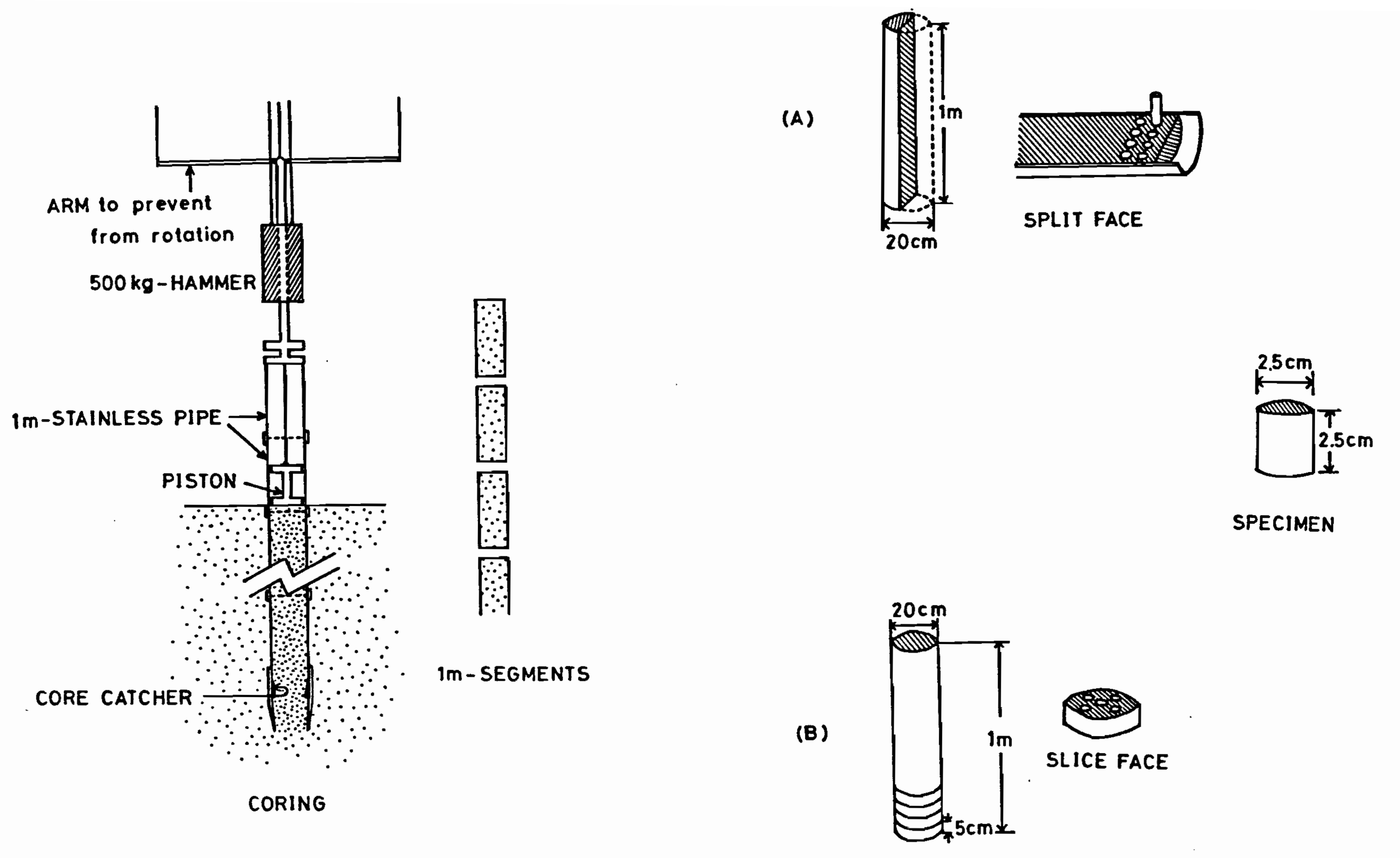

Fig.6 A sampling procedure showing from coring with a giant piston corer (left) to preparation of specimens (right). Two methods of types A and B were taken for the preparation of specimens : type A for the cores OS1, OS2, MZ1 and YG1, and type B for the cores OS3, HR1 and KZ3.

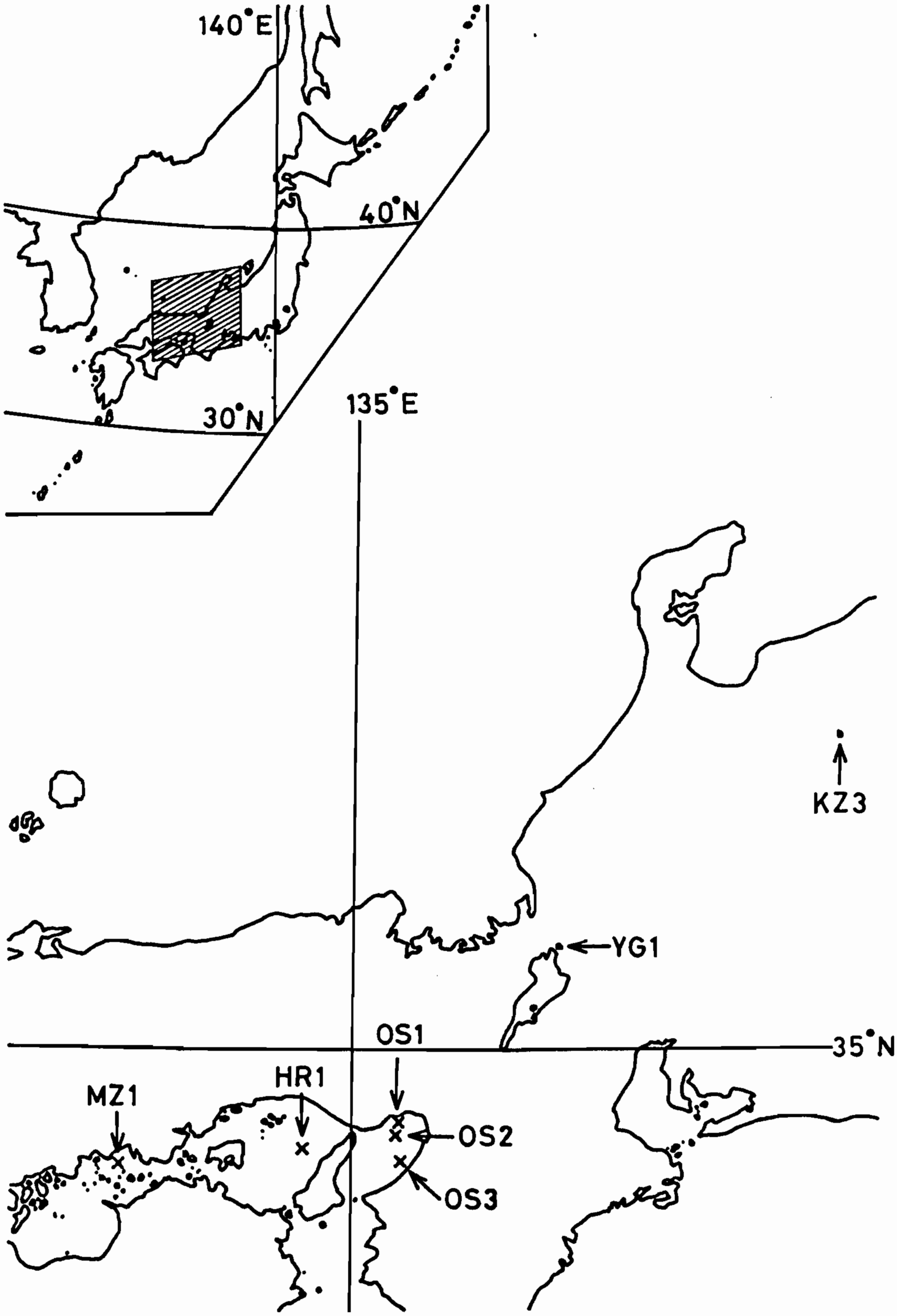

Fig. 7 Location map of the seven core samples from central to south-western Japan. Sampling places are streched over Osaka Bay (OS1, OS2 and OS3), Harima-nada (HR1), Mizushima-nada (MZ1), Lake Yogo (YG1) and Lake Kizaki (KZ3).

interpreted as a trace of transgression (Hyodo & Yaskawa, 1984a). The two cores of lacustrine deposits consist of clay and organic material. The core YG1 is almost composed with very fine inorganic clay slightly including organic material. On the contrary, the core KZ3 shows a complex stratigraphy. The upper half consists of pollen and other finely disseminated organic debris and the lower half is the laminae of the organic material and inorganic clay.

Magnetization was measured with a super-conducting magnetometer whose sensitivity is 10^{-8}emu. After measurement of natural remanent magnetization (NRM) of all specimens, saturation isothermal remanent magnetization (SIRM) given in a steady field of 3000 Oe was measured with respect to a specimen per depth level. Magnetization of all the cores was measured with wet specimens immediately after sampling except the core OS1. With respect to the core OS1, however, magnetization was measured with semi-dried specimens after stored in the laboratory for 5 years. The results of the measurements are shown in Fig.8. Declinations are relative ones whose overall mean is set to zero. Each core sediment has a characteristic record of magnetization. For example, the core HR1 displays very smooth change of magnetization direction, while the remanence of the core MZ1 changes in direction with very large amplitude. In order to express comprehensively the characteristic features of magnetization, several kinds of mean values for each core are listed in Table 1. Mean inclinations ($\bar{I}$) of all the cores are close to the inclination of a geocentric axial dipole field at the sampling site, 54.0° except the core MZ1. The core MZ1 has

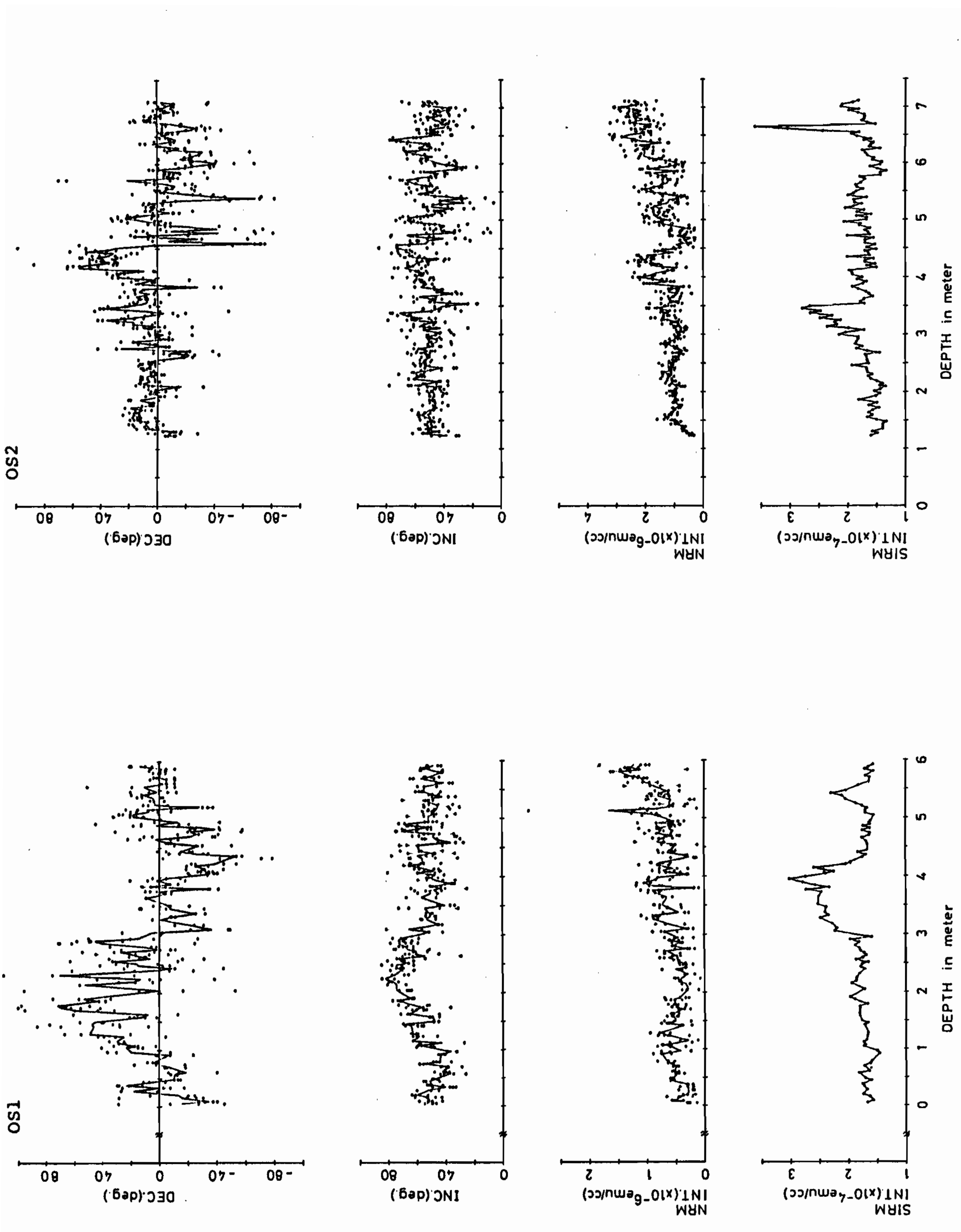
OS1
OS2
DEC.(deg.)
INC.(deg.)
NRM
INT.(x10-6emu/cc)
SIRM
INT.(x10-4emu/cc)
DEPTH in meter

Fig.8

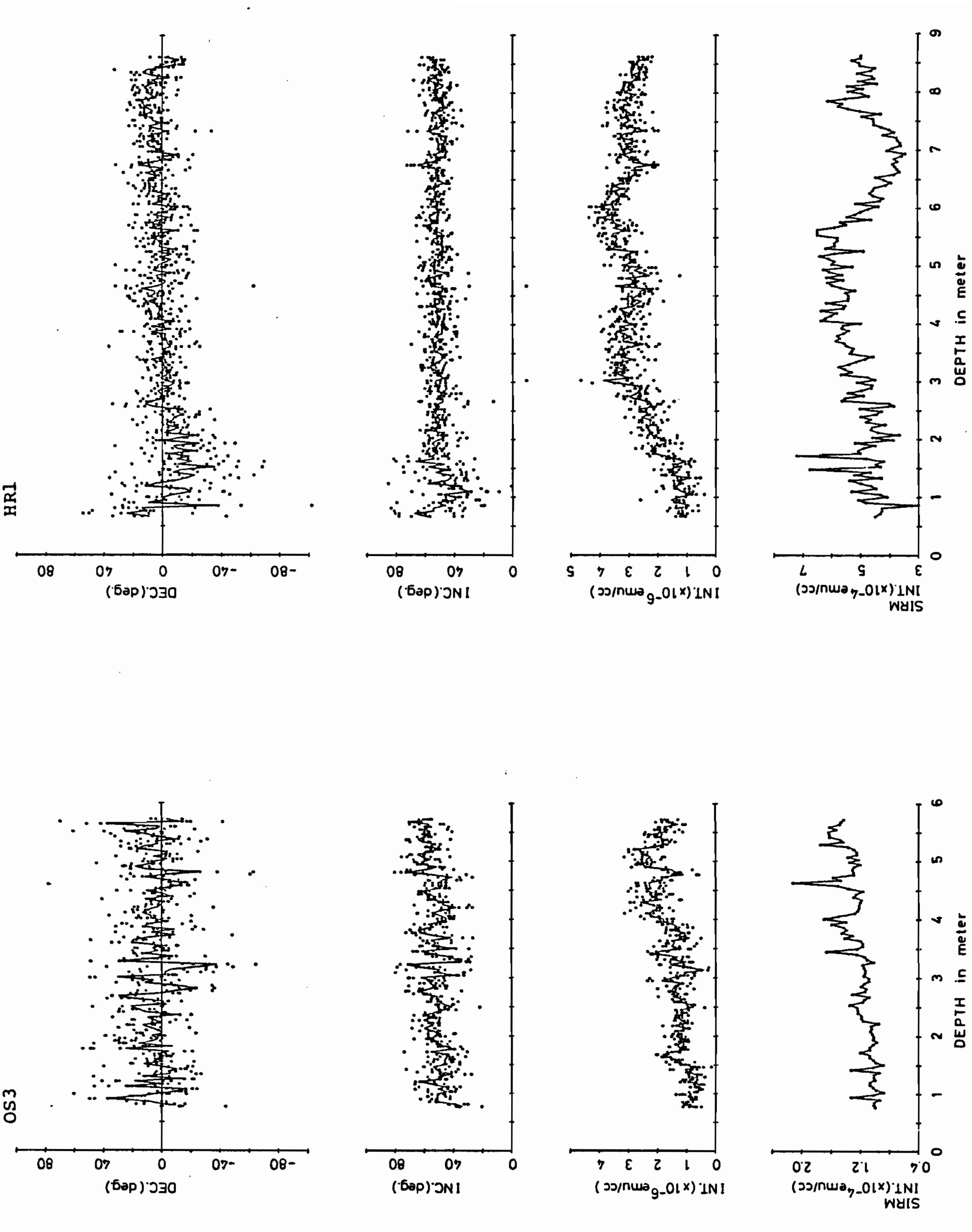
HR1
OS3
DEC.(deg.)
INC.(deg.)
INT.(x10^-6 emu/cc)
SIRM
INT.(x10^-4 emu/cc)
DEPTH in meter

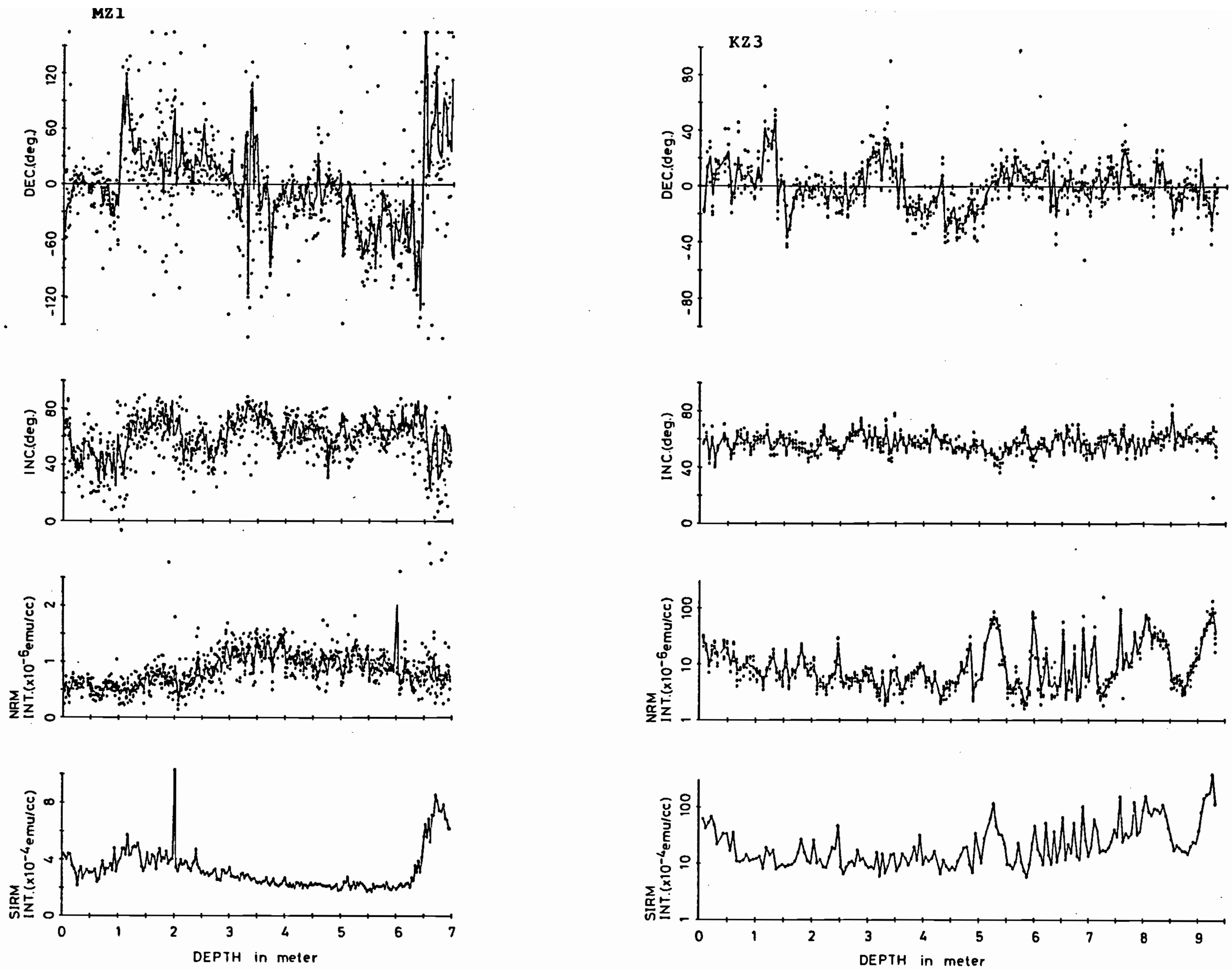
MZ1
KZ3
DEC.(deg.)
INC.(deg.)
NRM
INT.(x10^-6 emu/cc)
SIRM
INT.(x10^-4 emu/cc)
DEPTH in meter

Fig.8

Fig.8 Declination, inclination and intensity of NRM (upper three), and SIRM intensity (bottom). Dots show data of all specimens. Solid lines are drawn mean values in each depth level. The SIRM intensity show the value on a specimen per depth level.

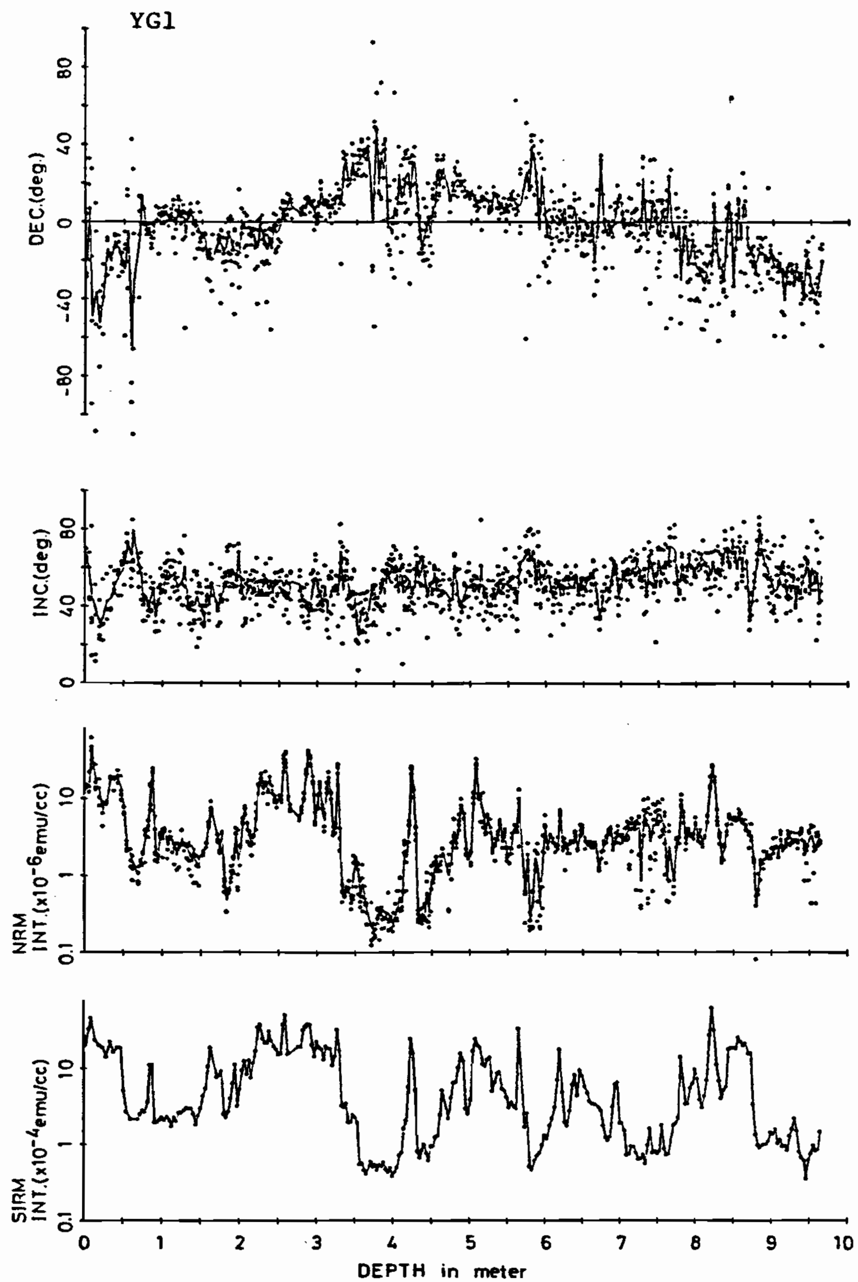

Sampling place	Core	Length (m)	Number of sampling horizons	Material	Overall mean values					
					$\overline{I}$ (deg)	$\overline{\alpha_{95}}$ (deg)	$\overline{SIRM}$ ($\times 10^{-3}$ (emu/cm^3)	$\overline{\rho_b}$ (g/cm^3)	$\overline{Am}$ (deg.)	$\overline{Z_{1/2}}$ (cm)
	OS1	6.0	106	clay	57.4	13.4	1.88	1.47	15.4	——
Osaka Bay	OS2	7.1	155	clay	52.3	12.9	1.76	1.49	13.2	4.0
	OS3	5.7	111	silty clay	53.4	11.8	1.23	1.43	9.3	14.0
Harima-nada	HR1	8.6	177	silt	51.6	9.7	4.99	1.65	6.1	68.0
Mizushima-nada	MZ1	7.4	225	clay	66.7	20.3	3.24	1.55	18.0	3.6
Lake Yogo	YG1	9.7	295	clay	54.2	11.8	8.04	——	11.9	6.5
Lake Kizaki	KZ3	9.3	173	organic clay	58.5	5.5	31.4	1.22	8.3	30.0

$\overline{I}$; mean inclination

$\overline{\alpha_{95}}$; mean α_{95} confidence circle

$\overline{\rho_b}$; mean bulk density

$\overline{Am}$; mean directional amplitude

$\overline{Z_{1/2}}$; mean half fixing depth

Table 1. Description of characteristic features for the seven core-sediments.

an abnormally high $\overline{I}$, 66.7°. Dispersion of remanence direction is different with cores. The core KZ3 has the minimum dispersion. Its mean 95 % confidence circle ($\overline{\alpha_{95}}$) is only 5.5°, which is about a half of other cores' $\overline{\alpha_{95}}$. Considering that another lake-sediment core YG1 has a large $\overline{\alpha_{95}}$, the small dispersion of remanence of KZ3 may be caused by difference in material rather than difference in depositional environments. Sediment of KZ3 mostly consists of organic material, which is markedly reflected by small bulk density. Its mean bulk density ($\overline{\rho_b}$) is only 1.22 g/cm^3. The core KZ3 has an abnormal value in mean SIRM intensity ($\overline{SIRM}$), too, which is extremely large. The most scattered values are found in the mean amplitude of magnetization direction ($\overline{Am}$), which is a mean distance of horizon mean directions from the overall mean direction. The three cores from Osaka Bay have similar values with respect to all of $\overline{I}$, $\overline{\alpha_{95}}$, $\overline{SIRM}$ and $\overline{\rho_b}$, but they have different $\overline{Am}$. The difference in $\overline{Am}$ appears to depend on none of other mean values. Some other factors to controle the amplitude of directional change should be considered. If all the magnetization records whose features are different among cores are explained by a consistent process of magnetizing, it will be possible to reconstruct a secular variation of the geomagnetic field from the records of individual cores.

7. Analysis of the magnetization records

7.1 Correlative changes within a core

Paleomagnetic experiments using the present core-sediments provide us several kinds of information on magnetization. Dispersion of magnetization direction in each depth level is one of them. Directional dispersion has been scarcely discussed in paleomagnetism with a core sample of sediment, since most cores are too small in diameter to provide sufficient specimens for statistical treatment. The first discussion on directional dispersion was made with the magnetization data of the core OS2, with a result that strong correlation was found among curves of directional dispersion, differential direction and remanent intensity (Hyodo et al., 1983). Now, we recognize the correlation concerning to other core data, too. The curve (a) in Fig.9 shows differential direction $|dA/dz|$, moving angle of magnetization direction in a unit depth calculated with horizon mean directions. The curve (b) in Fig.9 shows observed remanent intensity, intensity of NRM normalized by SIRM intensity. The curve (c) in Fig.9 shows precision parameter K, inversely proportional to the square of dispersion. To recognize objectively the correlativity among the three curves, cross correlation coefficients were calculated among them. Fig.10.1 shows the result of calculation on the data set of the core OS2. The cross correlation coefficient between $|dA/dz|$ and log(K), shown by the curve (a), represents strong negative correlation with a peak around zero lag. It indicates that the dispersion becomes large where the magnetization direction steeply changes with depth. The cross correlation coefficient between observed intensity and log(K), shown by the curve (b), represents strong positive correlation with a peak around zero lag. It indicates that the observed intensity drops where direction scatters. These two correlation patterns can be interpreted as a resultant effect of the integration of field variation as expressed by Eq.2 : Integration of the field whose direction steeply changes produces out dispersed alignments of magnetic moments, which cause large scattering of magnetization direction and remanent intensity drop due to cancellation of magnetic vectors aligned in opposite directions. Therefore the post depositional remanence has the pattern of cross correlation coefficients that the two cross correlation curves (a) and (b) swell like the shape of a spindle's section around zero lag as that of the core OS2 shows in Fig.10.1.

The above two cross correlation coefficients were calculated on the data set of other cores, too. The results, shown in Fig.10, reveal that most of the cores have the same spindle shape pattern of correlation like the core OS2. The pattern is seen in five cores OS2, OS3, HR1, MZ1 and KZ3. The core YG1 has the normal pattern in the correlation curve (a) but not in the correlation curve (b) and the core OS1 does not show such correlation pattern in both correlation curves (a) and (b). With respect to the core YG1, extremely high intensity around the depth 7.5 m indicates that the normalization by SIRM is inadequate so that the normal pattern is not shown in the correlation curve (b), the curve of cross correlation

Fig.9 Correlative variation curves in each core data. (a) Differential direction of magnetization |dA/dz|. (b) Observed intensity (OBS.INT.). (c) Precision parameter K of magnetization direction in each depth level. (d) Calculated intensity change due to only cancellation (CAL.INT.). Right figure is the half fixing depth used in the calculation. Each curve is smoothed by an operation of 5-points running mean.

(1)

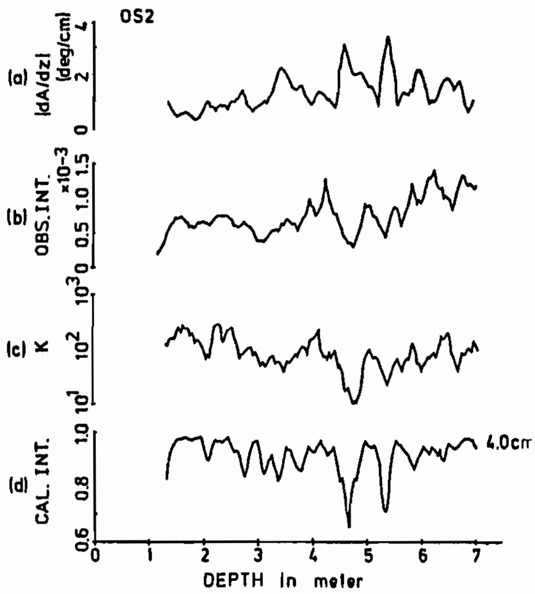

(2)

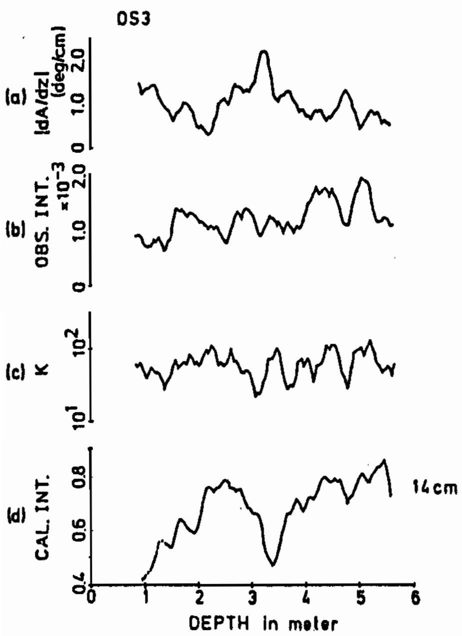

(3)

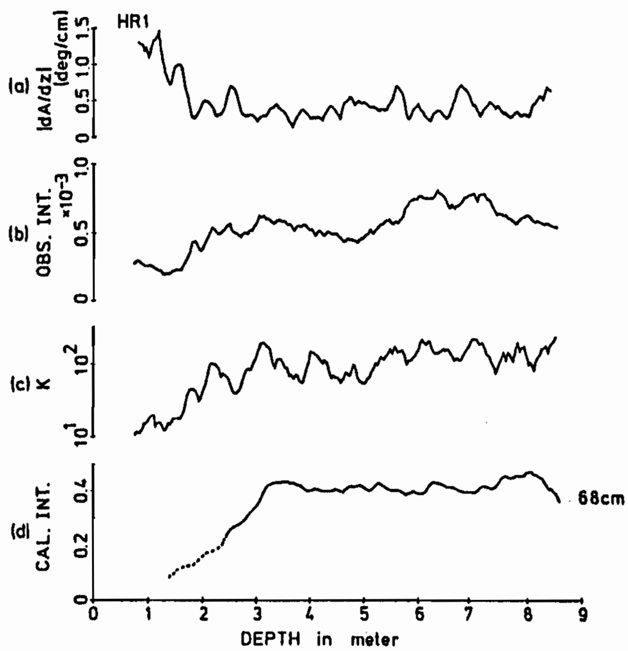

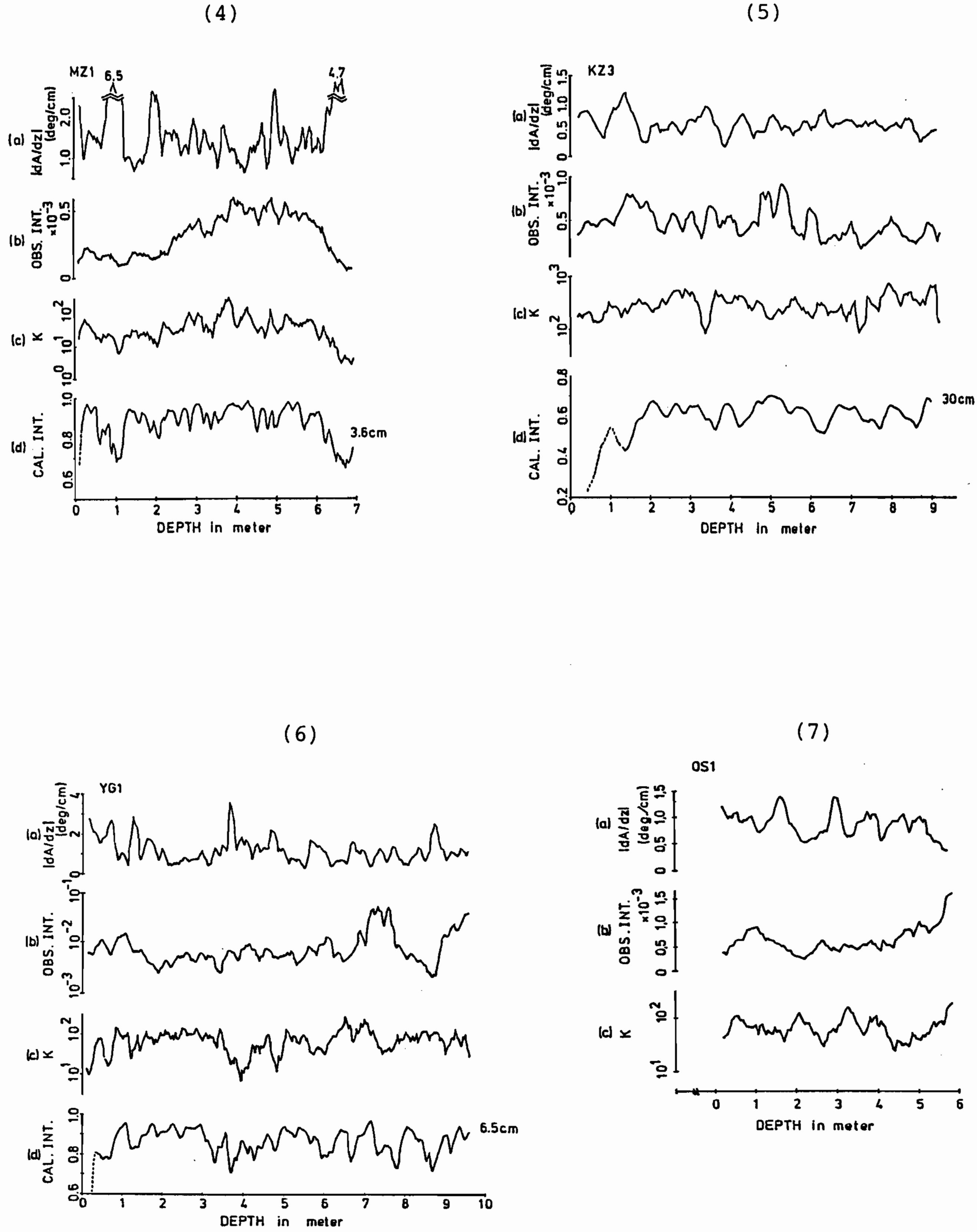
(4)
MZ1
6.5
4.7
(a) |dA/dz| (deg/cm)
(b) OBS. INT. ×10^-3
(c) K
(d) CAL. INT.
3.6cm
DEPTH in meter
(5)
KZ3
(a) |dA/dz| (deg/cm)
(b) OBS. INT. ×10^-3
(c) K
(d) CAL. INT.
30cm
DEPTH in meter
(6)
YG1
(a) |dA/dz| (deg/cm)
(b) OBS. INT.
(c) K
(d) CAL. INT.
6.5cm
DEPTH in meter
(7)
OS1
(a) |dA/dz| (deg/cm)
(b) OBS. INT. ×10^-3
(c) K
DEPTH in meter

Fig.9

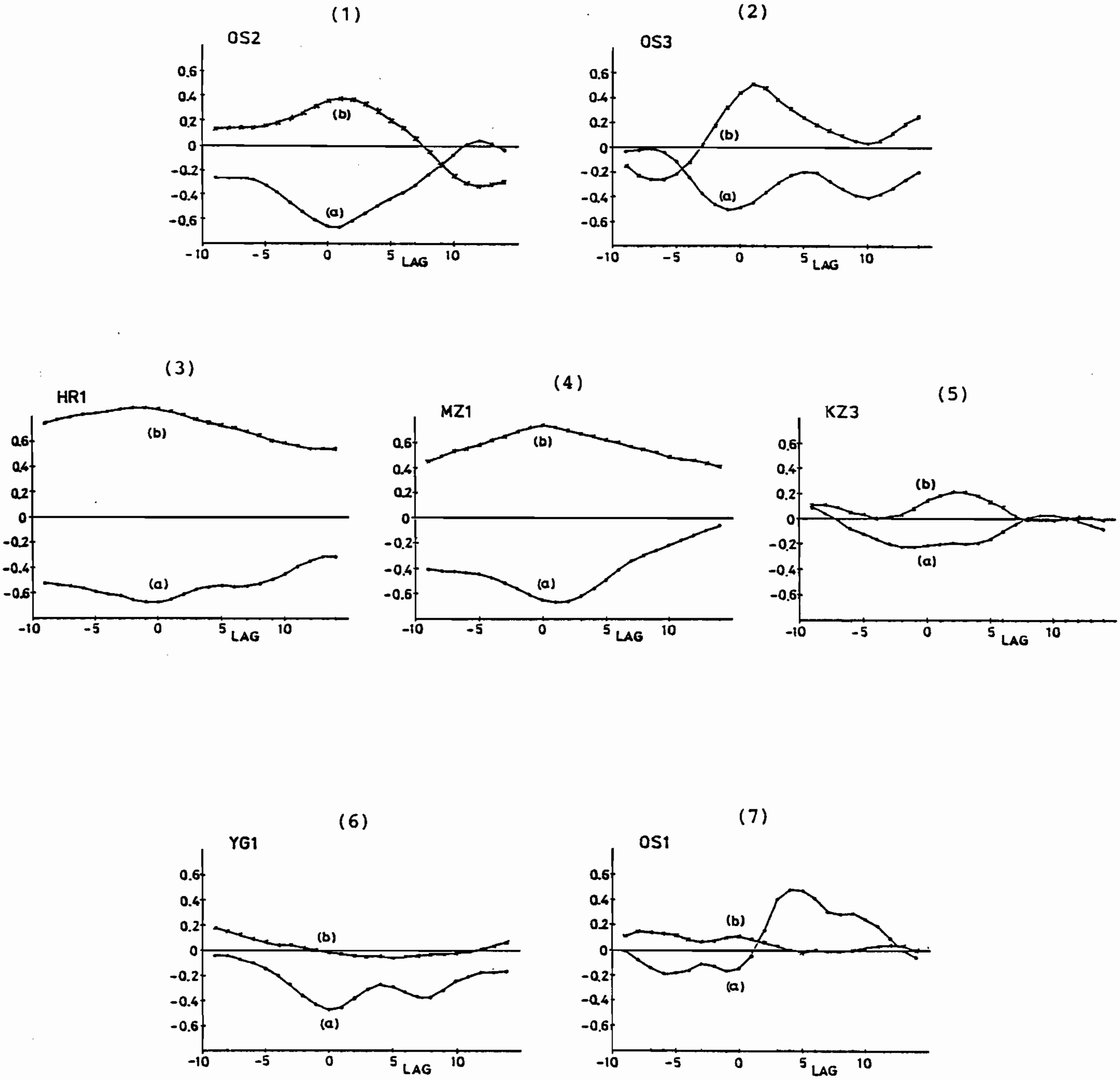

Fig.10 Correlation patterns among precision parameter K, differential direction |dA/dz| and observed intensity OBS.INT.. Curve (a) shows cross correlation coefficients of log(K)/|dA/dz|. Curve (b) shows cross correlation coefficients of log(K)/OBS.INT.. One division in lag corresponds to the width of sampling interval in each core presented in Table 1.

coefficients between observed intensity and log(K).

Declination and inclination curves of all the cores are correlated in Fig.11(a) and Fig.11(b). Those of the core MZ1 are the recalculated ones in the new coordinates that vertical axis in the core was rotated by 12.7° in a plane including the mean declination to adjust the mean inclination 66.7° of the core to the inclination of the axial dipole field at the sampling site, 54.0°. The rotation of frame is based on the assumption that the high inclination of MZ1 is caused by tilting. Pronounced features common in each curve are linked by broken lines considering the shape of the curves and ages. The curve correlation shows that magnetization direction changes of all the cores agree very well even in detailed features except those of the cores OS1 and HR1. The cores showing consistent directional curves are all the ones which have the normal pattern of correlation (a). Although the core HR1 have the normal pattern of correlation (a), it is difficult to correlate its features of directional change with other cores' because of its quite small amplitude of changes.

The observed intensity curves are correlated in Fig.11(c). The intensity curves of OS2, OS3, HR1 and MZ1, which have the normal correlation pattern (b), agree one another in general trend, although fine fluctuations do not coincide as well as directional curves. Three cores YG1, KZ3 and OS1 show inconsistent change curves of intensity. The cores YG1 and OS1 do not have the normal pattern in correlation (b). Although the core KZ3 has the normal correlation pattern (b), the degree of the correlativity is very low.

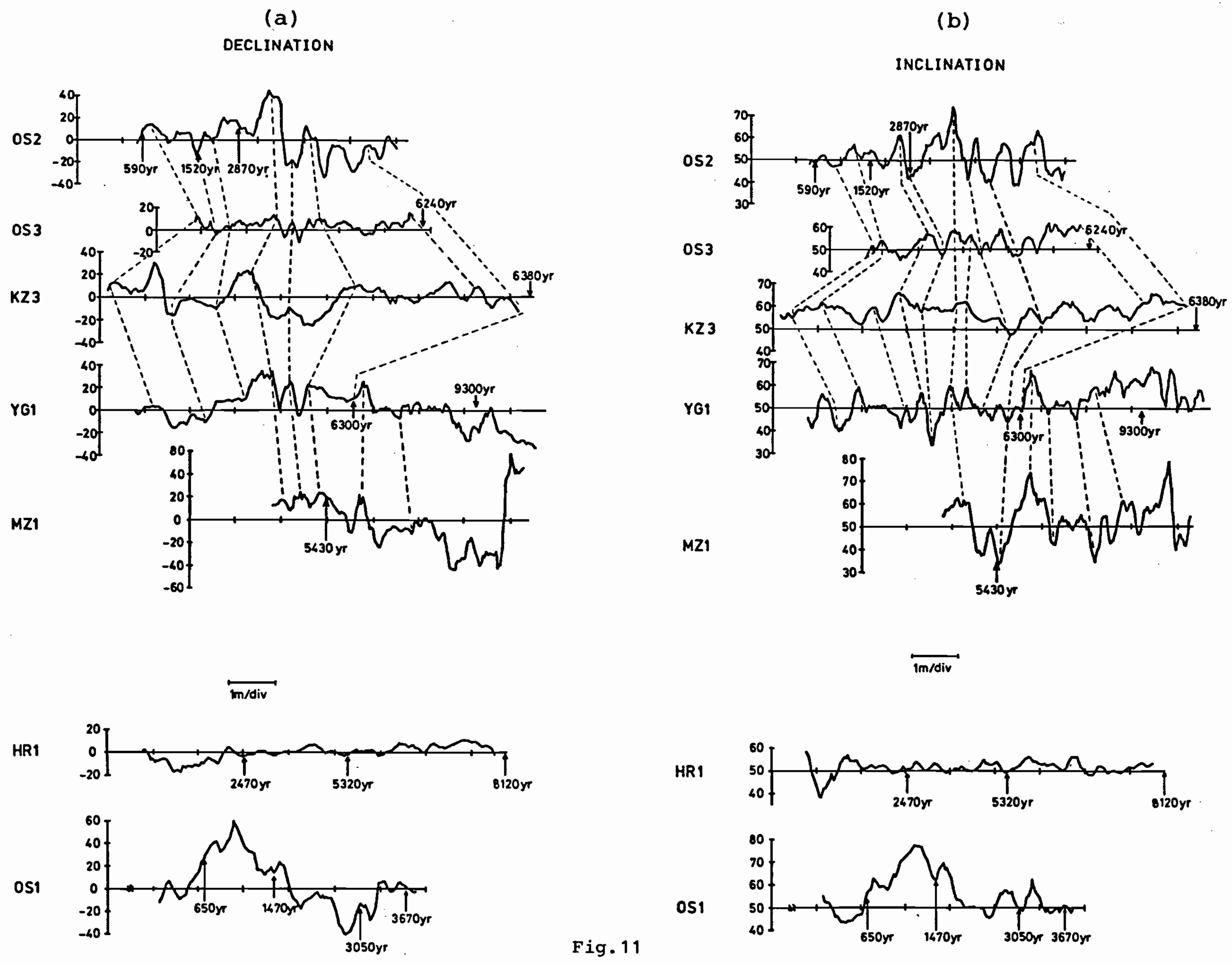
(a)
DECLINATION
OS2
OS3
KZ3
YG1
MZ1
HR1
OS1
40
20
0
-20
-40
-60
80
590yr
1520yr
2870yr
6240yr
6380yr
6300yr
9300yr
5430 yr
1m/div
2470yr
5320yr
8120yr
650yr
1470yr
3050yr
3670yr
(b)
INCLINATION
70
60
50
40
30
80

Fig.11

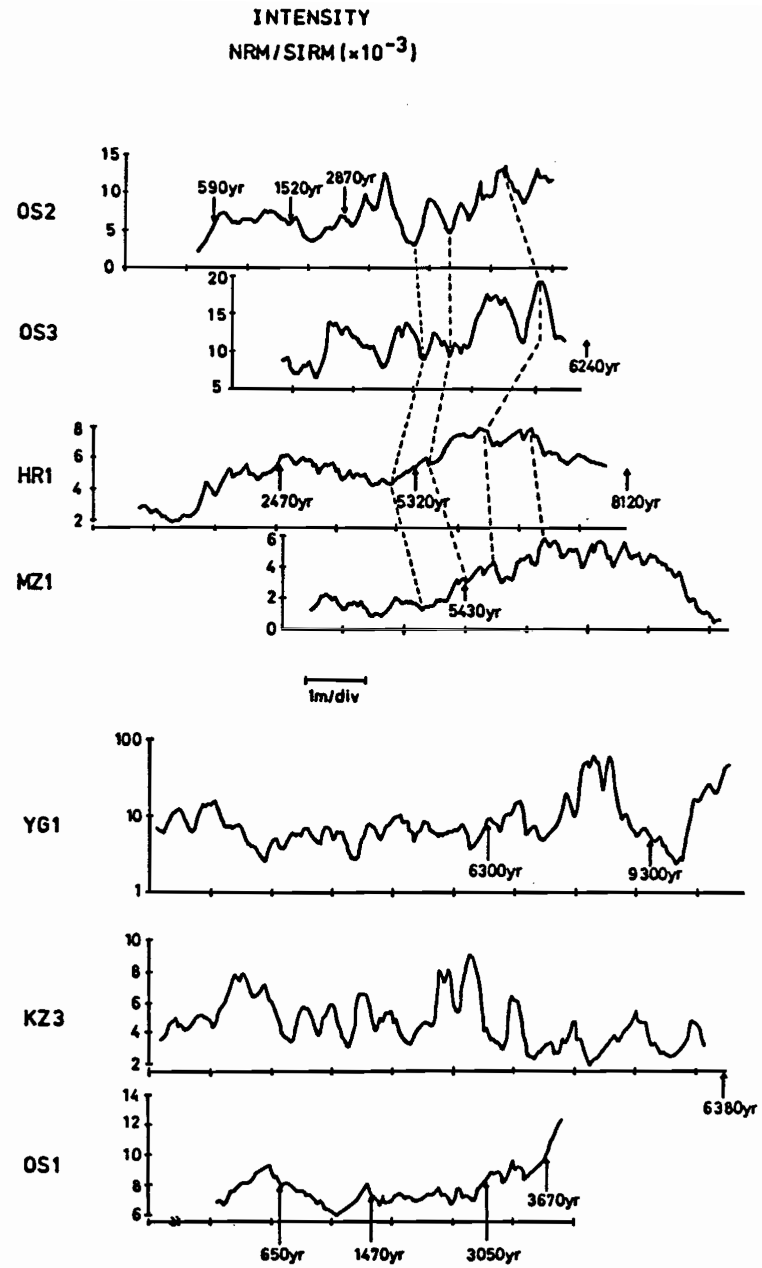

Fig.11 Comparison of (a) declination, (b) inclination and (c) NRM/SIRM intensity curves of each core. Common features among cores in each kind of curve are linked by broken lines in consideration of sediment ages besides the shape of the curves. The topmost disturved portions in YG1 and MZ1 are removed. Each curve is smoothed by an operation of 5-points running mean.

The above facts are summarized as follows : Magnetization data, which have the normal pattern in the correlation (a) between |dA/dz| and log(K), show consistent curves of directional variation. Magnetization data, which have the normal pattern in the correlation (b) between observed intensity and log(K), show consistent curves of remanent intensity changes. Thus remanent magnetization of core-sediments can be classified by the pattern of cross correlation coefficients. The correlation pattern appears to indicate the internal consistency of magnetization record.

7.2 Estimation of half fixing depth

The present model predicts the intensity decrease due to cancellation of magnetic moments aligned in various directions. Now, we estimate the intensity change using the linear system model with the magnetization direction for each core. The procedure of calculation is presented with the data set of the core OS2. The observed declination and inclination curves in Fig.12(a) must have been subjected to amplitude attenuation and phase shift passing through a filter of the moment fixing function. Therefore we first calculate a virtual secular variation of field direction from the magnetization direction by deconvolution. Eq.4 can be transformed as :

$$\mathbf{Fe}(\omega) = \mathbf{M}(\omega)/R(\omega) \qquad (9)$$

The field spectrum $\mathbf{Fe}(\omega)$ is obtained from the magnetization spectrum $\mathbf{M}(\omega)$ using Eq.9 and then the inverse Fourier transform of $\mathbf{Fe}(\omega)$ provides the virtual geomagnetic field secular variation

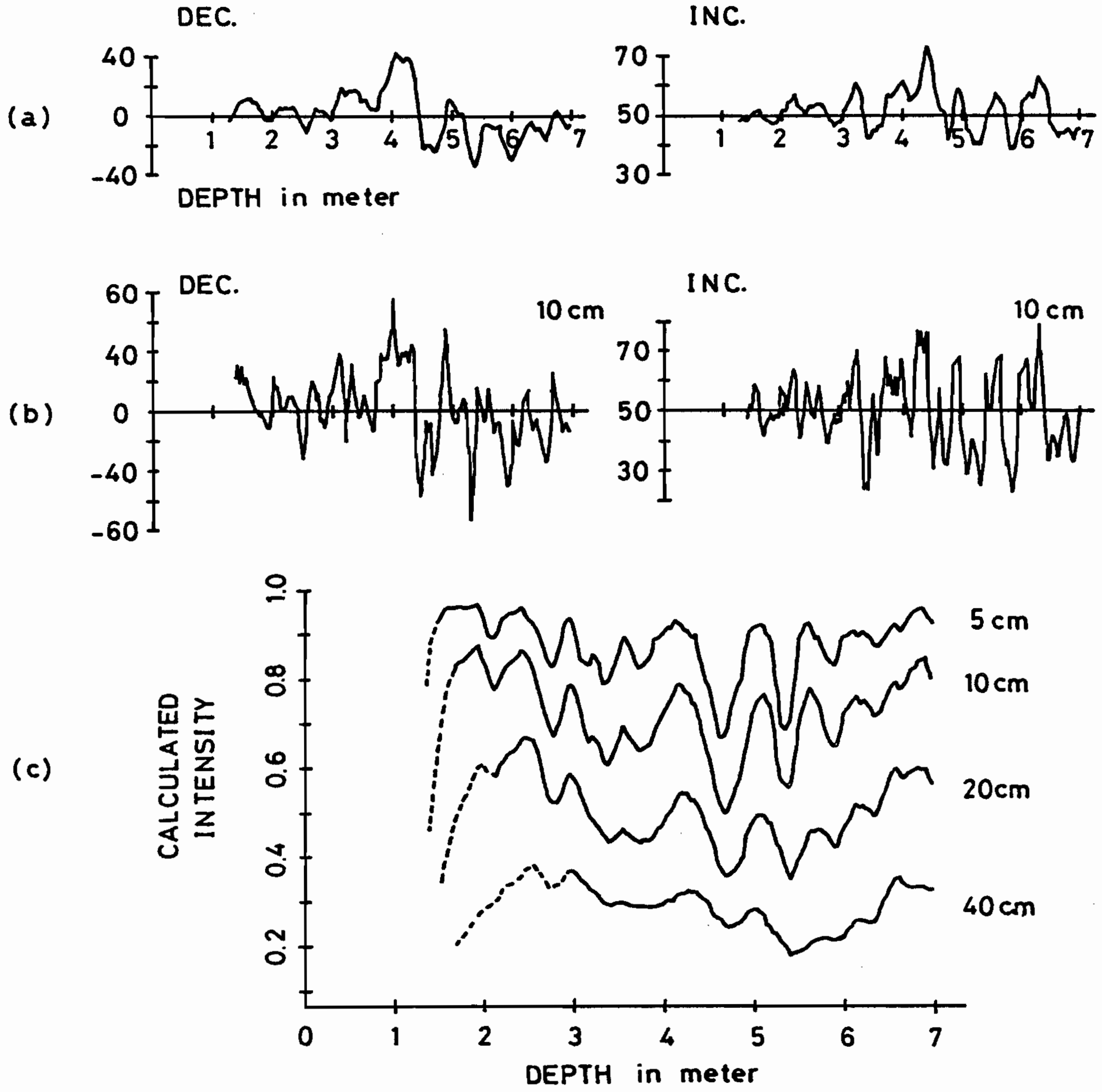

Fig.12 Calculation of the intensity reduction due to cancellation during a period with the same polarity. (a) Directional change of magnetizations in the core OS2. (b) Directional change of the virtual geomagnetic field variation deduced by a deconvolution with $Z_{1/2}$= 10 cm. (c) Intensity variations due to cancellation calculated with the virtual fields. The right figure shows $Z_{1/2}$ used in each calculation. (dotted line ; 50-95 % moment fixed, solid line ; over 95 % fixed) Each variation curve is smoothed by an operation of 5-points running mean.

fe(z) whose directional swings and fluctuations grow up. Through the operation of deconvolution all magnetization intensities were set to 1.0, and a depth axis was used instead of time. Fig.12(b) shows the virtual geomagnetic secular variation calculated by the above method with a filter of $Z_{1/2}$= 10 cm. Second, magnetization was calculated by the convolution integral of Eq.2 with the virtual geomagnetic secular variation and the moment fixing function determined by the same $Z_{1/2}$ with the one used in deconvolution. Intensities of virtual geomagnetic fields were again reset to 1.0. The variation curves of intensity due to only cancellation calculated with $Z_{1/2}$= 5, 10, 20 and 40 cm are shown in Fig.12(c). Some of them display very similar change curve to those of the precision parameter K and the observed intensity in Fig.9.1 Therefore cross correlation coefficient between each calculated intensity and log(K) was calculated to examine the correlativity. The result shows that higher correlation coefficients are calculated out on the $Z_{1/2}$ of some range than those with differentional direction $|dA/dz|$ and observed intensity NRM/SIRM.

The deconvolution in the above procedures of calculation should be carefully operated, since the $1/R(\omega)$ amplifies high frequency components. Although the spectra of Nyquist frequency and over were removed, noises are still amplified. We remove the high frequency components of the directional change of magnetization by an operation of 3-points running mean and recalculate the intensity change due to cancellation, as a result that correlation of the calculated intensity with log(K) drops suddenly. It is considered that high frequency change of field direction clearly plays an important role in the intensity reduction due to cancellation. Hence, the deconvolution was made using the original magnetic data without any high-cut operation.

The above calculations were carried out on every core data. Fig.13 shows curves of the cross correlation coefficient at zero lag between log(K) and calculated intensity with respect to various $Z_{1/2}$. Every curve except that of the core OS1 has a peak at a certain $Z_{1/2}$. Even the cores KZ3 and HR1, which show quite weak correlation, have peaks. Fig.9(d) represents the calculated intensity curve which shows the highest correlation with log(K). It is the best fitting curve to the observed intensity, too.

The $Z_{1/2}$, with which the intensity change best correlated with changes of log(K) and observed intensity is calculated, was related to the average amplitude of directional change $\overline{Am}$ presented in Table 1. The $\overline{Am}$ for each core is plotted to the $Z_{1/2}$ deduced above, in Fig.14. Probability of the $Z_{1/2}$ is presented by a horizontal bar, width of $Z_{1/2}$ showing more than 98 % peak value for cross correlation coefficient in Fig.13. The average amplitudes are ordered by the $Z_{1/2}$, being consistent with the amplitude attenuation predicted from the model in Fig.3 ; the larger the $Z_{1/2}$, the more the amplitude is attenuated. Considering that each sediment has almost equal rate of deposition and records a secular variation of the same time span, the estimates of $Z_{1/2}$ are reasonable enough to explain the amplitude difference by the difference of filtering effect. The $Z_{1/2}$ deduced above appears to be regarded as a rough estimate for the average half fixing depth $\overline{Z_{1/2}}$ throughout the core length. Magnetization data of the core OS1, which have

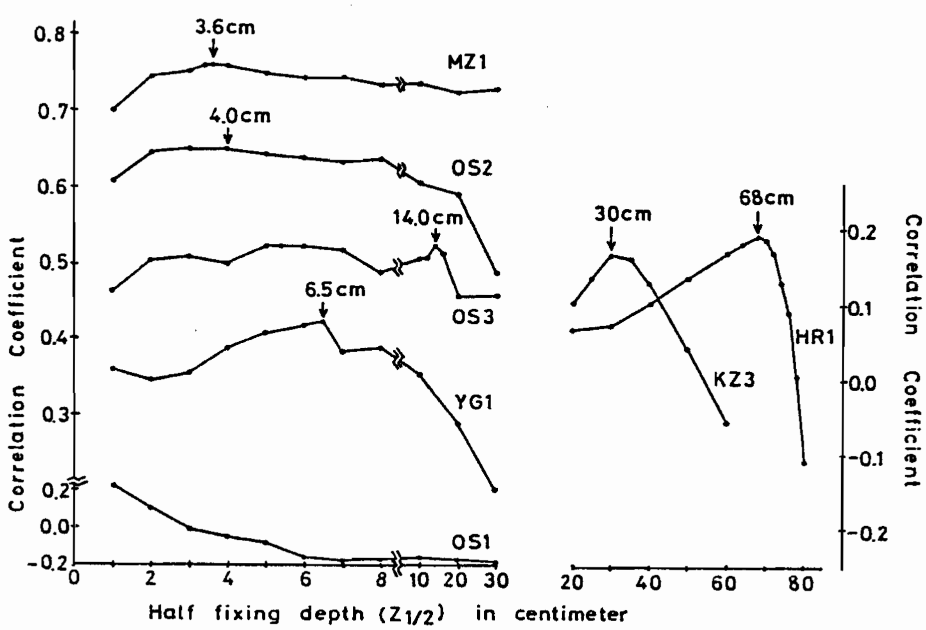

Fig.13 Cross correlation coefficients between K and calculated intensity of various $Z_{1/2}$. The place of the highest correlation is shown by an arrow and a value of $Z_{1/2}$ for each core.

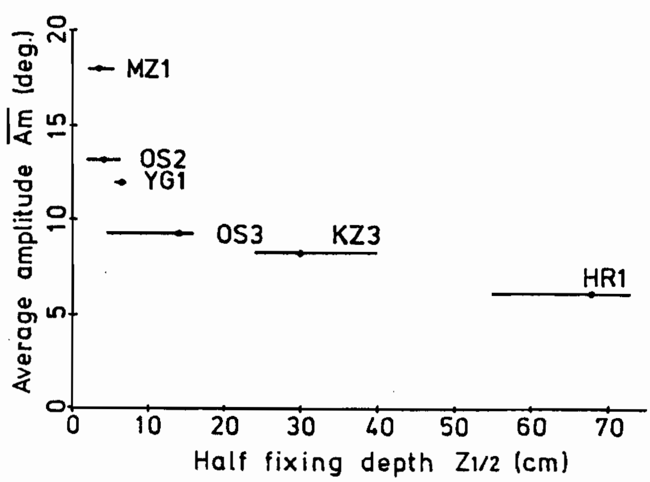

Fig.14 Relation between the average amplitude of directional change $\overline{Am}$ and the half fixing depth $Z_{1/2}$ obtained in Fig.13. The horizontal bar shows width of the $Z_{1/2}$ showing the correlation more than 98 % peak value for cross correlation coefficient in Fig.13. Compare with the amplitude attenuation due to filter in Fig.3.

independent correlation pattern among K, |dA/dz| and observed intensity (Fig.10), do not show positive correlation between calculated intensity and log(K), too. Consequently, the average half fixing depth could not be obtained for OS1 by the above method.

7.3 Deconvolution

Curve correlation of declination and inclination in Fig.11 shows that each curve is similar in shape, possessing same swings in contemporary portions, but amplitude of the swings is different with cores. The difference can be ascribed to the filtering effect by moment fixing function with different $Z_{1/2}$, expressed by Eq.7. Now, we try to remove the effect by deconvolution. The deconvolution was carried out with Eq.9, using data set of only declination and inclination as done in chapter 3. We did not use intensity data, since they do not show consistent changes so well as those of declination and inclination. The average half fixing depth $\overline{Z_{1/2}}$, deduced in chapter 9, was used throughout core length.

Results of the deconvolution are shown in Fig.15. Topmost disturved portions in the cores MZ1 and YG1 have already removed before the operation of deconvolution (Fig.11). Swings of small amplitude in the cores possessing large $Z_{1/2}$ are amplified by deconvolution to have the amplitude as large as that of the cores with small $Z_{1/2}$, as a result that the amplitude difference among cores disappears. Especially, the directional curve of HR1, which is almost flat before deconvolution, is changed so largely

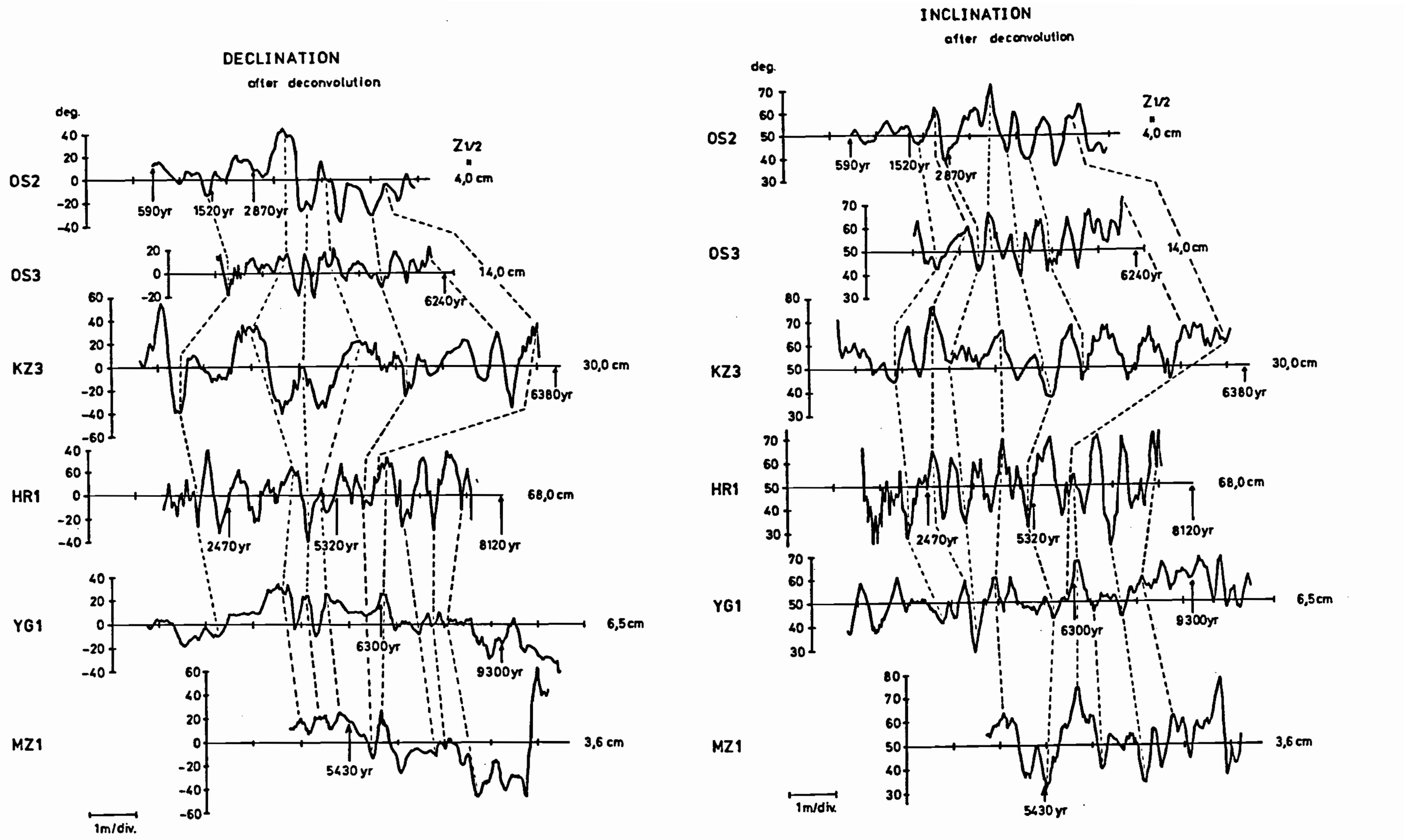

Fig.15 Comparison of (a) declination and (b) inclination curves after deconvolution for each core. Right figures show half fixing depths used in deconvolution. Each curve is operated with 5-points running mean.

that major swings existing in all other cores grow up to be recognizable. There are some abnormal fluctuations of high amplitude in the curve of HR1, which may be attributed to amplified noises or fluctuations by the edge effect. There is no conspicuous phase shift due to deconvolution. Especially, curves of OS2, YG1 and MZ1, whose half fixing depths are less than 10 cm, show quite small shift in phase. They show quite small change in amplitude, too.

Declination and inclination curves before deconvolution could be intercore correlated in only shape of swings. On the other hand, curves after deconvolution could be correlated fitting swings even in absolute value. This fact exactly indicates that the past geomagnetic field is reconstructed by the operation of deconvolution.

8. Alternating field demagnetization

Alternating field (AF) demagnetization tests were made on pilot samples for each core, using a demagnetizor with field rotating system (Matsuda, et al., 1981). According to the results, remanent magnetization of most of cores is stable, but that of the cores HR1 and OS3 is unstable. Especially the remanence of the core HR1 widely moves in direction after demagnetization at each step displaying its peculiar movement, which differs from that of thermal remanent magnetization of volcanic rocks.

Results of stepwise AF-demagnetization with peak fields of 50, 100 and 150 Oe on pilot sets of specimens from depths 217 cm (HR711) and 517 cm (HR411) in the core HR1 are shown in Fig.16. Most of specimens have their median destructive fields (MDF) between 100 and 150 Oe. Remanence directions of all specimens in both horizons largely move after each step of demagnetization. However, their movements after AF-demagnetization appear to have common tendency within each horizon. They shift in parallel with each other ; remanences of specimens in HR711 show clockwise shift and those in HR411 straight eastward shift. They do not converge as the peak field is increased. Although most of specimens in other pilot horizons also represent such a pattern after AF-demagnetization, specimens of some horizons show distinct patterns, e.g. some of them have very stable remanences scarcely move in direction or others have unstable ones radially disperse as a peak field is increased. The unstable remanence of the core OS3 also show the same behavior to AF-demagnetization,

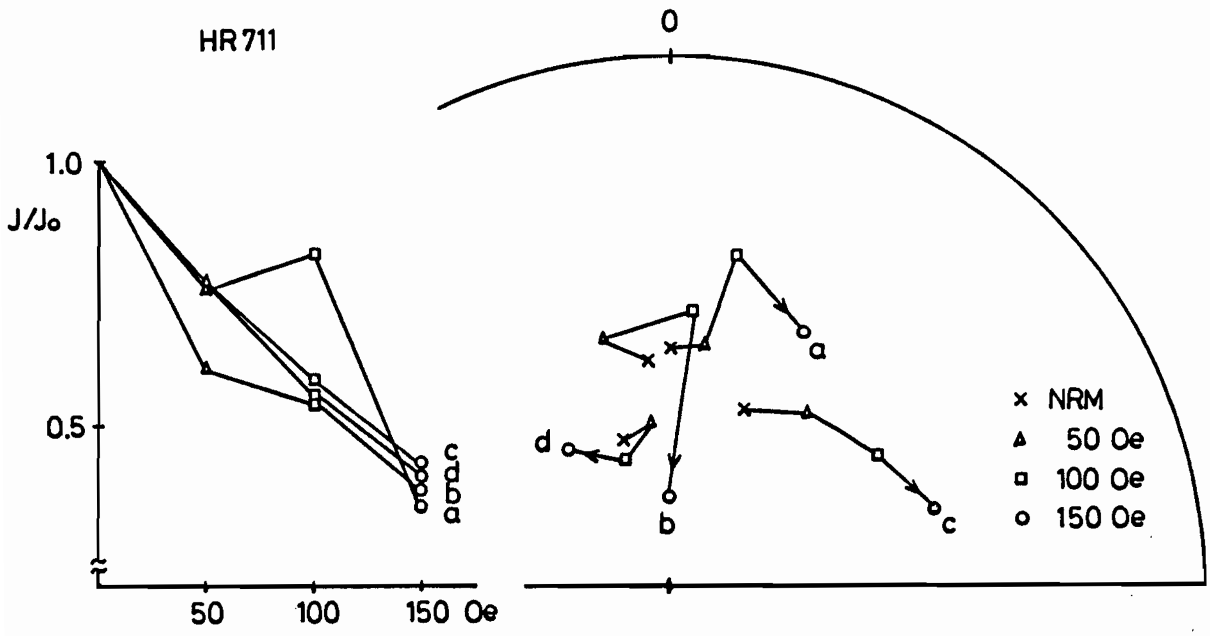

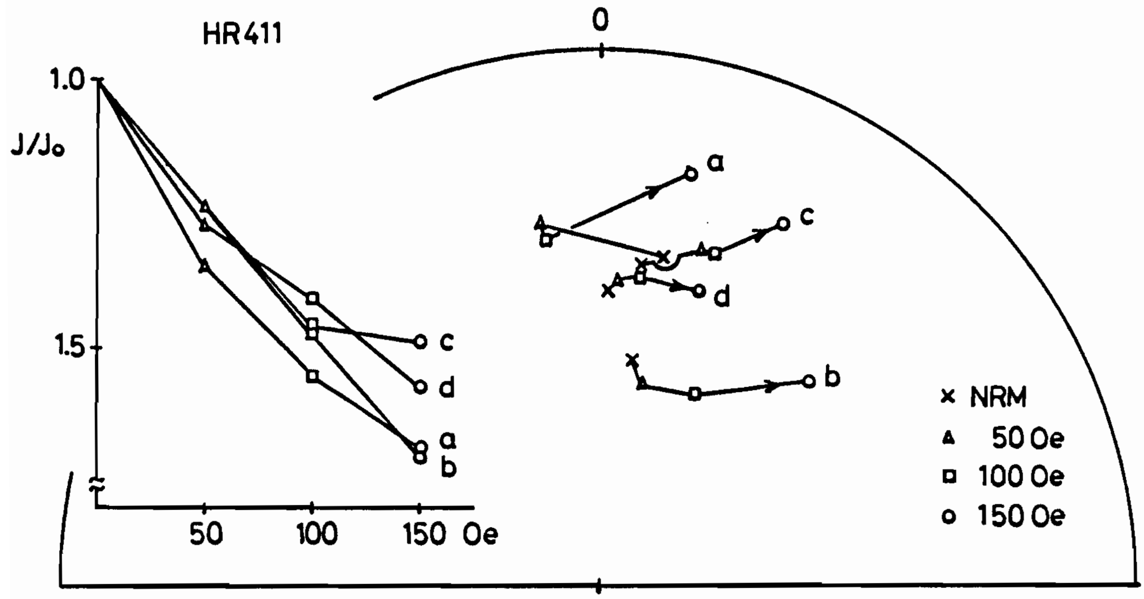

Fig.16 Results of stepwise AF-demagnetization at fields of 50, 100 and 150 Oe on pilot samples from the same age horizon in the core HR1. The two results are from depth levels of 217 cm (HR711) and 517 cm (HR411).

although the shifting distance of direction is much smaller than that of HR1.

A series of 79 specimens of the core HR1, selected every other horizon except the top loose section 165 cm, were stepwise demagnetized in alternating fields of 50, 100 and 150 Oe. The results are shown in Fig.17. Although flat curves of declination and inclination of NRM begin to swing after the demagnetization in a field of 50 Oe, and gradually grow up with the peak field increased. This phenomenum is similar to that of deconvolution. Fig.18 shows change of the direction curve of HR1 after deconvolution with $Z_{1/2}$ of 20, 40 and 60 cm. The deconvolution gives rise to swinging and fluctuating in the smooth declination and inclination, and the amplitude of the swings increases with $Z_{1/2}$, as the phenomenum by AF-demagnetization in Fig.17, although detailed swings are not shown in the curve after demagnetization because of its poor resolution of the 10cm-intervals. We further demagnetized 78 specimens in the remaining horizons every 10 cm in a field of 150 Oe, too, and compare the directional curve of the remanence every 5 cm after 150 Oe-demagnetization with that after deconvolution with $Z_{1/2}$= 60 cm (Fig.19). They show very similar changes in both declination and inclination. High frequency changes especially clustered in inclination, which could be even considered to be excessively amplified by deconvolution, correspondingly coexist in the two curves. These phenomena of demagnetization, which appears to be equivalent to the deconvolution, may impose some restrictions upon a model of the magnetizing process of sediments, along with the parallel shifting of remanence directions.

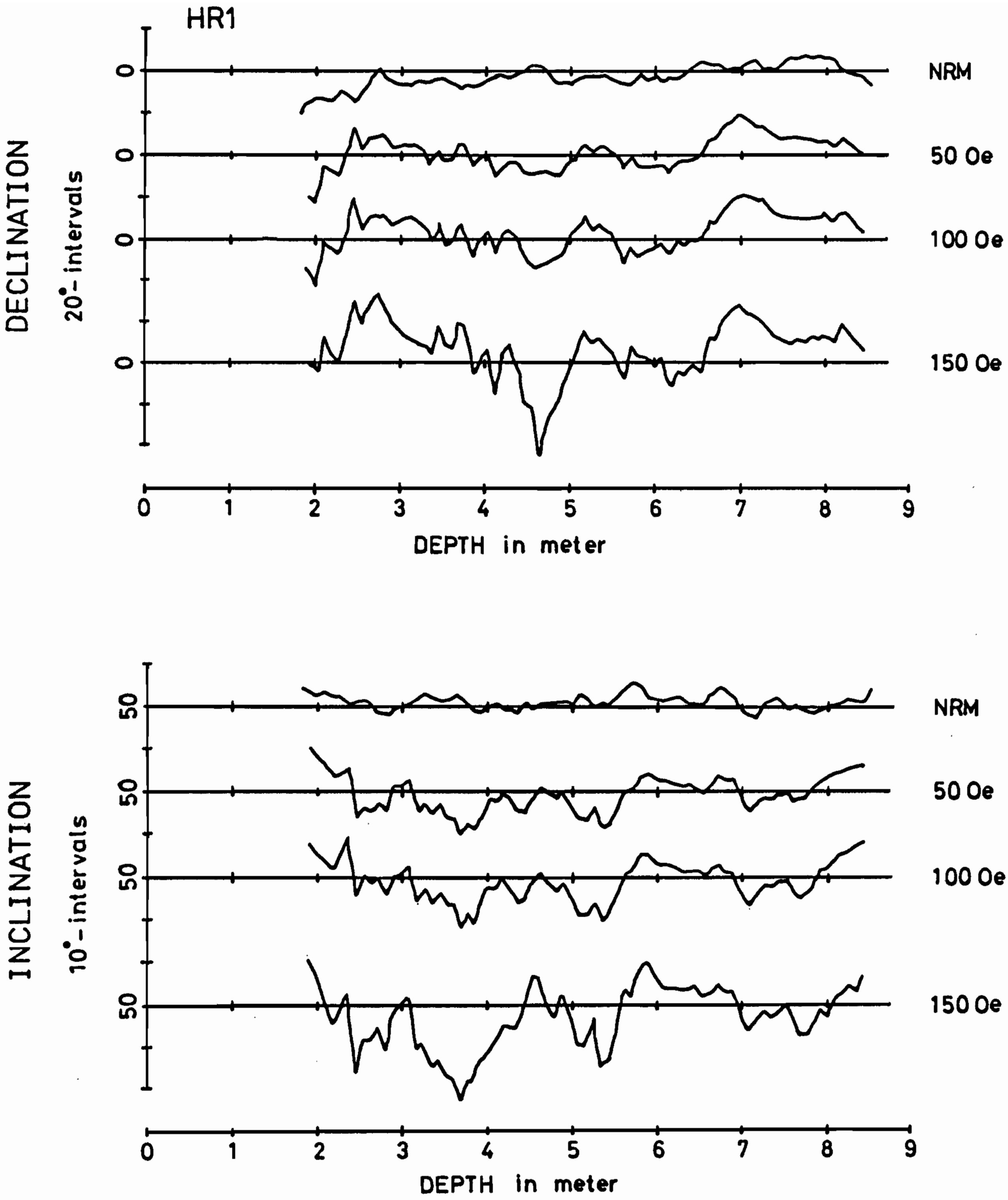

Fig.17 Gradual change of declination and inclination curves in the core HR1 after stepwise AF-demagnetization at fields of 50, 100 and 150 Oe, using a serial samples every 10 cm. Each curve is smoothed by an operation of 5-points running mean.

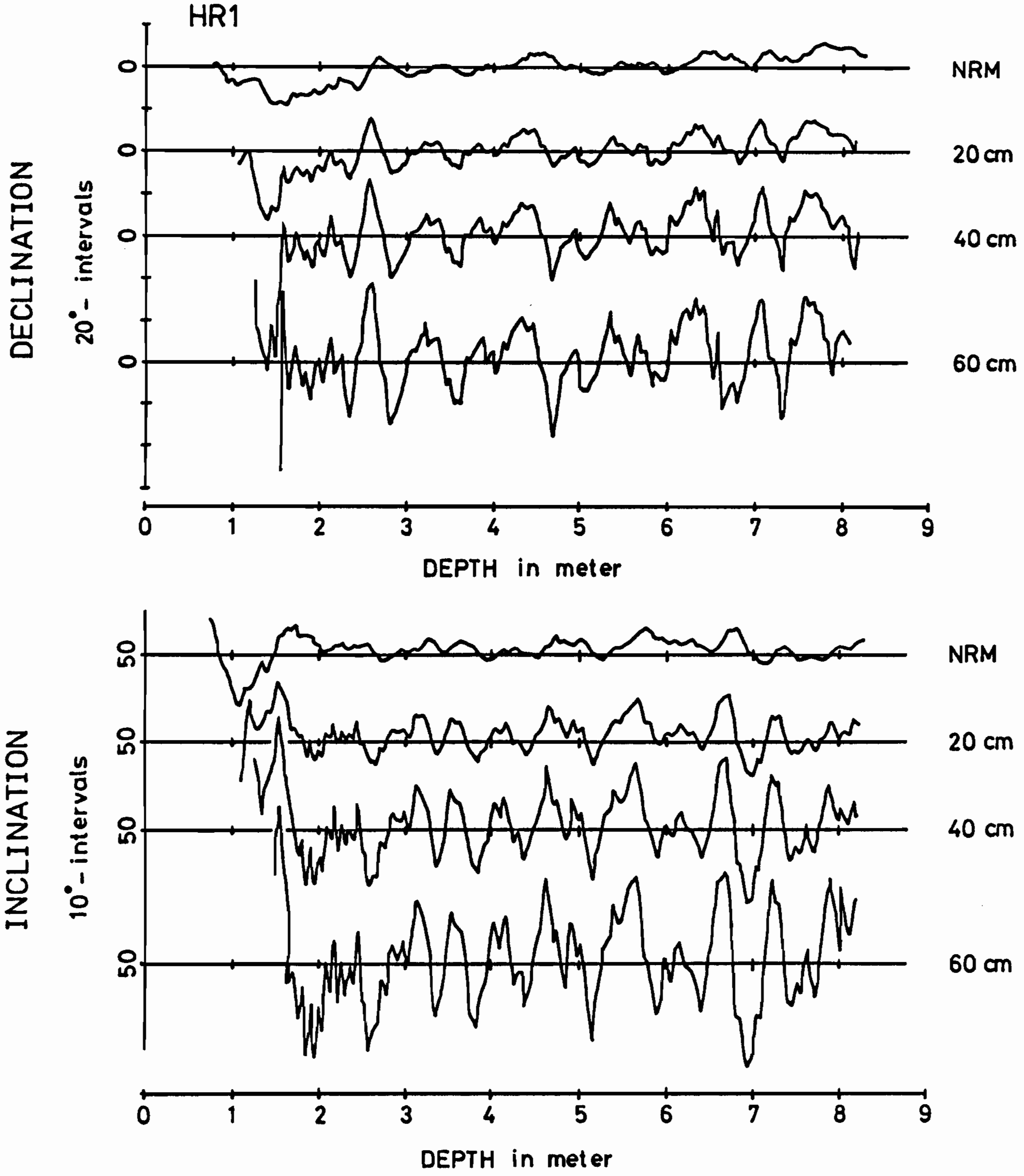

Fig.18 Gradual change of declination and inclination curves in the core HR1 after deconvolution with $Z_{1/2}$ = 20, 40 and 60 cm, using mean NRM directions every 5 cm. Topmost section corresponding to the length of $Z_{1/2}$ in each curve is removed. Sections of 30 cm at both ends, abnormally fluctuated by edge effect, are further removed, too. Each curve is smoothed by an operation of 5-points running mean.

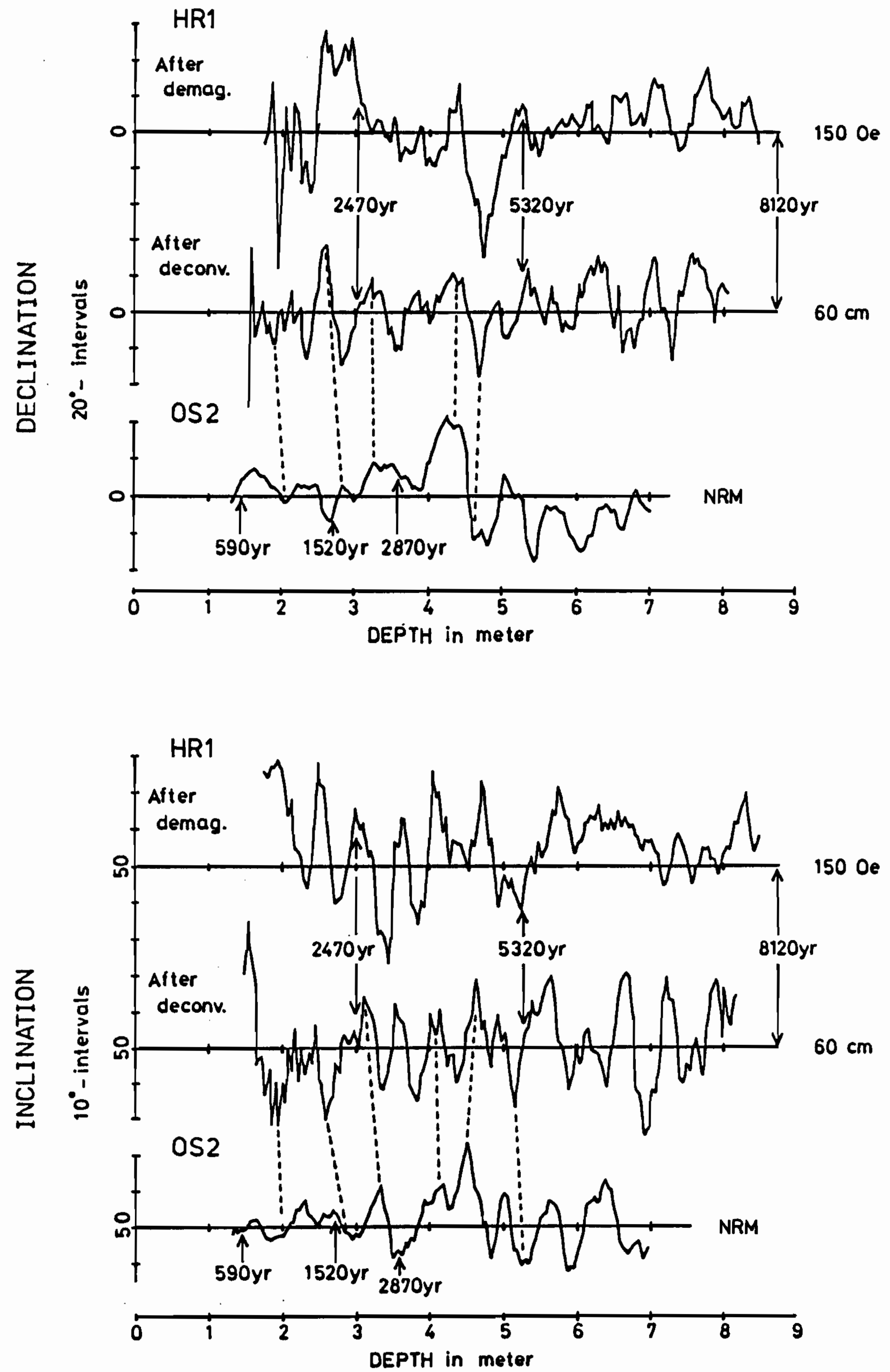
HR1
After demag.
150 Oe
2470yr
5320yr
8120yr
After deconv.
60 cm
DECLINATION
20°- intervals
OS2
NRM
590yr
1520yr
2870yr
0 1 2 3 4 5 6 7 8 9
DEPTH in meter
HR1
After demag.
150 Oe
2470yr
5320yr
8120yr
After deconv.
60 cm
INCLINATION
10°- intervals
OS2
NRM
590yr
1520yr
2870yr
0 1 2 3 4 5 6 7 8 9
DEPTH in meter

* Fig.19

It is further shown in Fig.19 that they agree with the directional change of the NRM in the core OS2, whose $Z_{1/2}$ is so small that its remanence direction can be regarded as the exact direction of the past field being subjected to little filtering. As shown by linking common swings with broken lines in Fig.19, they show high degree correspondence in both declination and inclination, especially over the time span from about 1000 years B.P. to 5000 years B.P.. Considering that the portion for the last 2000 years in the declination and inclination of OS2 is well consistent with the archeomagnetic one (Hyodo & Yaskawa, 1980), it is regarded that the geomagnetic secular variation can be deduced from the magnetization of HR1 through the operation of deconvolution and also AF-demagnetization.

---

* Fig.19 Consistent change curves of declination and inclination in the core HR1 after demagnetization in a field of 150 Oe and after deconvolution with $Z_{1/2}$ = 60 cm. They are further correlated with the directional curve of the NRM in the core OS2. Each curve is smoothed by an operation of 5-points running mean.

9. Secular variation of field direction

A secular variation curve of the past geomagnetic field in the Holocene time can be obtained from the remanence of the present core-sediments. We do not stack the magnetization records because their quality is different with cores as shown by the internal consistency of magnetization (Fig.10). Stacking may cause fading-out of detailed features in the records of high quality. We discuss the variation curve of declination and inclination in the core OS2 as a standard curve judged from the following criteria. (i) Half fixing depth is small. (ii) Remanent magnetization shows high internal consistency : Strong correlation exists among K, differential direction, observed intensity and calculated intensity. (iii) Mean inclination is close to the expected value of a geocentric axial dipole field.

9.1 Determination of age axis

Only three ages of sediment are obtained in the core OS2. We try to move the ages in other cores presented in Fig.11 to the corresponding depths of OS2 by correlating magnetic curves in order to construct a detailed depth-age relation of OS2. Two ages of 6300 and 9300 years B.P. were determined in the core YG1 by identifying tephras to be Akahoya and Utsuryo-to from refractive index of volcanic glass (Arai, 1981). Other ages are all determined by ^{14}C-dating. Seven ^{14}C-ages in the cores OS1, HR1 and MZ1, and an age of tephra in the core YG1 were added to the age axis of OS2 as magnetic ages. The curve correlation for dating was made with declination and inclination for all cores except the core OS1. The declination and inclination curves after deconvolution (Fig.15) was used to correlate for the core HR1 and the directional curve of NRM was used for other cores (Fig.11). The ages in OS1 were moved correlating SIRM curves, since the cores OS1 and OS2 show similar SIRM curves. The similarity reflects that they have almost the same sequence of material, for they were taken at almost near places in 1 km. Eleven ages listed in Table 2 are plotted on to the depth of OS2 in Fig.20. They show a curved line like the letter 's' not an exponential one in assumption that homogeneous sediment are deposited at a uniform rate (Yaskawa, 1973). Ages between data points are determined by linear interpolation.

9.2 Age plots of declination and inclination

Fig.21.1(a) shows age plot of declination and Fig.21.2(a) shows that of inclination for the core OS2. These can be regarded as those of secular variation of the geomagnetic field, since they have been subjected to little deformation by filtering because of its small $\overline{Z_{1/2}}$, 4.0 cm. Detailed characteristic features of the past geomagnetic field through back to 7000 years B.P. are well presented by the OS2 data. Swings in both declination and inclination are named for the convenience of later discussion. Initials 'D' and 'I' represent swings of declination and inclination, respectively. Upward swings are expressed by odd numbers and downward swings by even numbers. The numbering starts with the youngest swing in the

Depth in OS2 (cm)	Age (years B.P.)	Dating method	Correlation curve	Core
144 ± 27	590 ± 80	^{14}C	————	OS2
165	650 ± 80	^{14}C	SIRM int.	OS1
260	1470 ± 125	^{14}C	SIRM int.	OS1
269 ± 15	1520 ± 85	^{14}C	————	OS2
330	2475 ± 125	^{14}C	Dec. & Inc.	HR1
357 ± 19	2870 ± 90	^{14}C	————	OS2
375	3050 ± 80	^{14}C	SIRM int.	OS1
412	3670 ± 65	^{14}C	SIRM int.	OS1
520	5320 ± 190	^{14}C	Dec. & Inc.	HR1
530	5430 ± 80	^{14}C	Dec. & Inc.	MZ1
630	6300	Tephra	Dec. & Inc.	YG1

Table 2. Ages of depths in the core OS2. In addition to three ages determined in OS2, eight ages in other cores are brought to corresponding depths in OS2 by correlating declination and inclination curves, or SIRM-intensity curves.

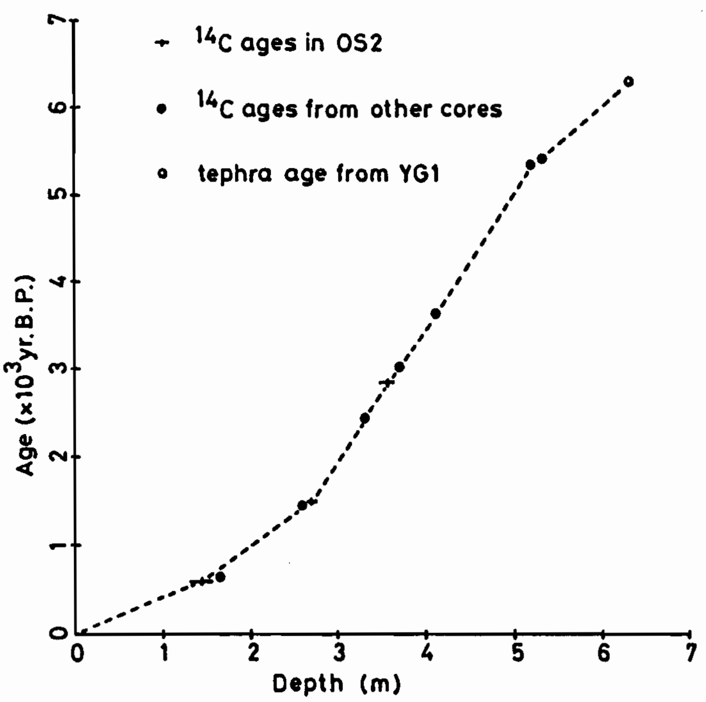

Fig.20 Depth-age relation of the core OS2. Symbols are ages in Table 2. Depths between data points are dated by a linear interpolation as shown by the dotted line.

(1) DECLINATION

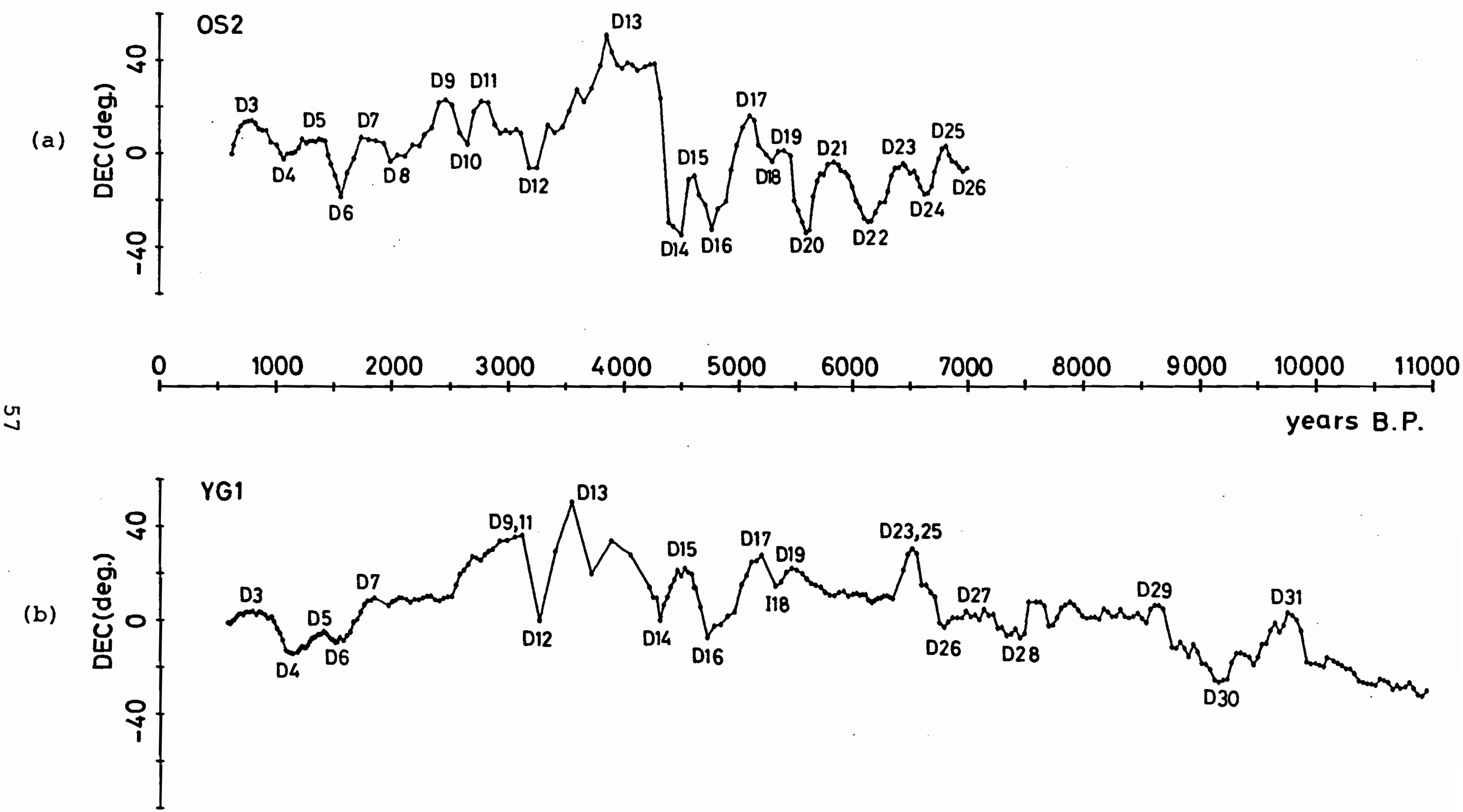

Fig.21 The secular variation of the geomagnetic field for the last 11000 years in south-western Japan. Dots show the direction after the operation of 150-years running mean. Swings are named with combinations of initials 'D' or 'I', and numbers.

(2) INCLINATION

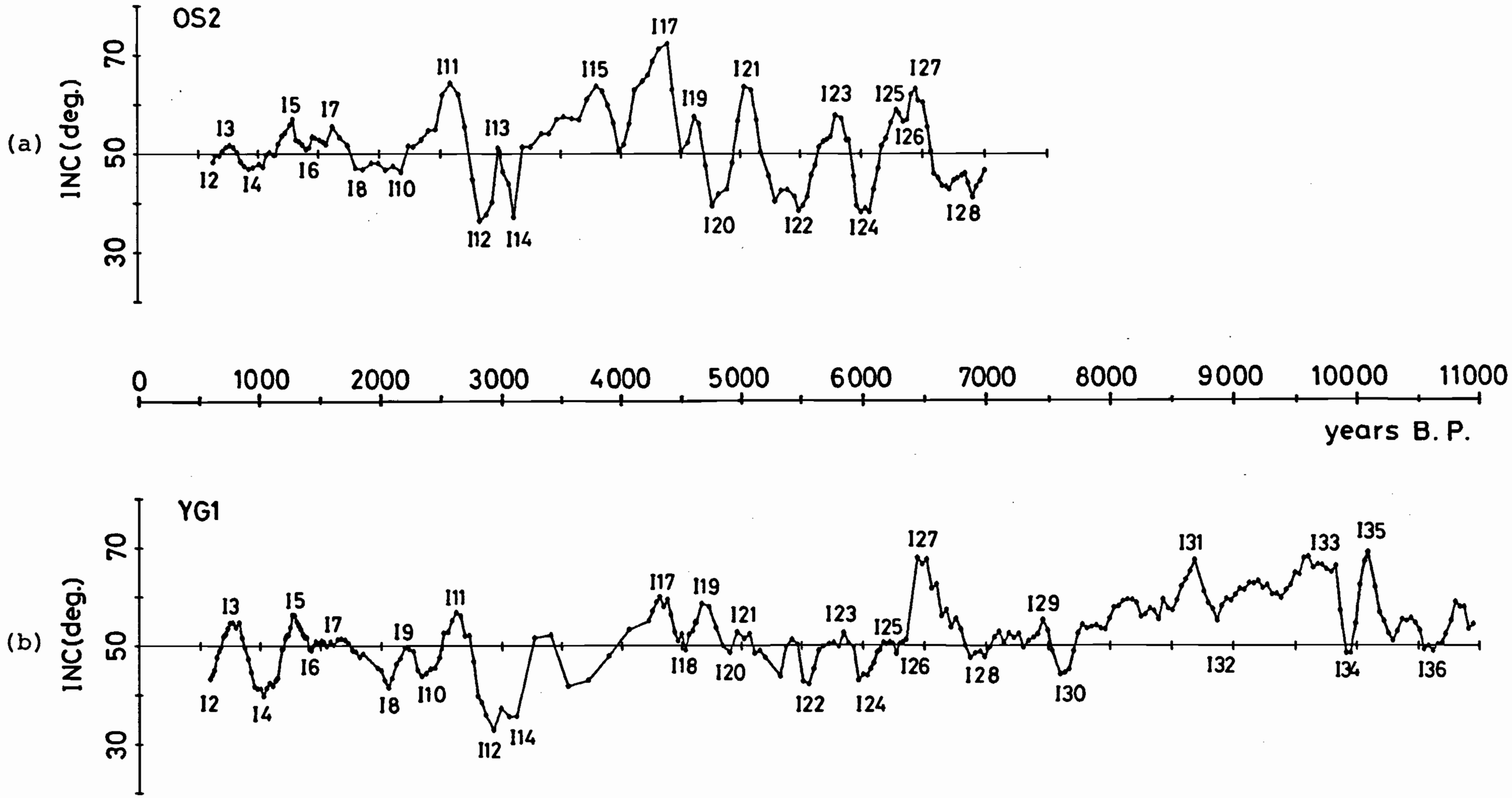

Fig.21

archeomagnetic curve in Fig.22. Declination and inclination of the core YG1 was plotted to age axis in order to extend the time span of secular variation of the geomagnetic field. The data for the core nearly meet the criteria as a standard curve. The core has two ages by tephrochronology, 6300 and 9300 years B.P. and the bottom age is estimated to extend beyond 10000 year B.P.. Data of depth-age relation were increased by correlating swings of YG1 with the dated swings of OS2. The age axis of YG1 was constructed by linear interpolation of dated depths for the period after 9300 years ago and by extrapolation with the trend between the depths of 6300 and 9300 years B.P. for the period before 9300 years ago. According to the extrapolation, the bottom age of the core YG1 is 11000 years B.P.. Declination and inclination of YG1 is plotted to the age axis in Fig.21.1(b) and Fig.21.2(b), respectively.

9.3 Comparison with archeomagnetic data

The topmost portion for the last 2000 years of the declination and inclination curves in the core OS2 is correlated with the secular variation from archeomagnetism (Hirooka, 1971) in Fig.22. Crosses and solid circles of OS2 in Fig.22 show NRM direction of each specimen and mean value in each depth level, respectively. The archeomagnetic field directions are shown by solid circles with error bars and the broken line is drawn on mean direction every 50 years, in Fig.22. Each swing in the archeomagnetic curve has a corresponding swing in the OS2 curve. Comparison of the two data reveals that the directional variation

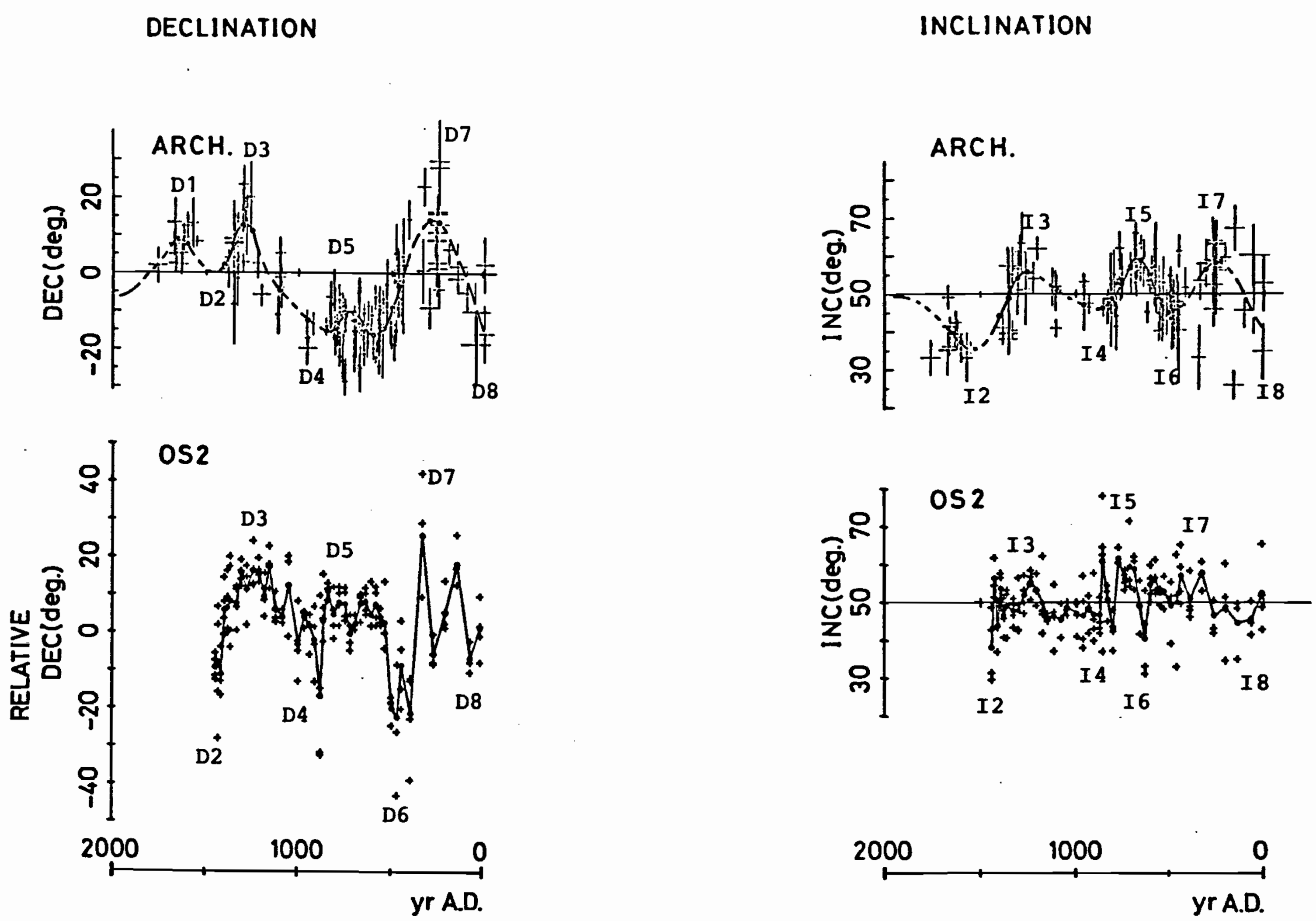

Fig.22 Declination and inclination of the geomagnetic secular variation from archeomagnetism (after Hirooka, 1971) and in the core OS2. Crosses show individual data points. The broken line in the archeomagnetic plots and the solid line in the OS2 plots show means of every 50 years and each level, respectively. Each swing is named as in Fig.21.

of OS2 rather agree well with the variation of the archeomagnetic data-points than the smoothed curve by the broken line. Only discrepancy is in the swing D6 : the pronounced westerly swing D6 in the declination of OS2 does not exist in the archeomagntic declination. There is little difference in phase between the two curves. It is thus independently verified by the agreement with the archeomagnetic data that the half fixing depth of the core OS2 is very small so that the geomagnetic field variation is faithfully recorded in its remanent magnetization.

9.4 Behavior of field direction

Long wavelength changes in the past geomagnetic field is as follows. Declination of the field largely deviates westwards about 11000 years ago. The field turns eastwards through 7000 years and has the most easterly declination around 4000 years ago. After that it starts turning westwards, again. Inclination suddenly rises up to about 70° around 10000 years ago, and since then gradually becomes shallow through 7000 years. After it has the lowest value about 30° about 3000 years ago, it immediately restores and keeps its average about 50° up to present.

The core MZ1 has an unconformity at the depth 6.9 m, where material of the sediment changes from bottom sand to upper clay and the declination suddenly shifts westward about 80°. According to the correlation with the remanence direction of the oriented samples of shallow water sediments from the mouth of Samondo River, Osaka Bay (Muroi & Yaskawa, 1977), the unconformity is caused by a hiatus longer than 3000 years due to the sea level change and the age of the upper side of the boundary is about 8000 years B.P. (Hyodo & Yaskawa, 1984a). The discrepancy in declination indicates the time gap between the Holocene transgression and the former one, and suggests that the geomagnetic field about 8000 years ago has the declination swinged westerly by 80° from that of the field at the former transgression. This verifies that the large westerly declination before about 8000 years ago which is also observed in the core YG1 is the exact behavior of the geomagnetic field not the one by twisting of the sediment column and so on.

There are a number of short wavelength swings, which seems to be able to be used for age determination. The most prominent feature, which should be the most suitable for dating, exists about 4400 years ago (2400 years B.C.), where the inclination has an extremely high peak (I17) and the declination suddenly shifted largely from west to east (D14 & D13).

10. Discussion

10.1 Significance of the formulation

The present model is characterized by a moment fixing function. Although the function was expressed by an exponential one determined by a half fixing depth $Z_{1/2}$ in the present study, it may take other forms. For example, the Dirac's δ function is possible if all magnetic particles in a horizon are simultaneously fixed, or it may not show a monotonous decrease but any others like bimodal changes. But no experimental result which suggests these functions has been obtained. Therefore, it is at present reasonable to approximate by an exponential function based on results of laboratory experiments.

It is considered that fixing of magnetic grains, which determines a moment fixing function, is controled by a size distribution of magnetic and non-magnetic grains, their shape, magnetization intensity of them, property of interstitial fluid, sedimentation rate, and intensity of geomagnetic field. All but the last two factors show physical properties of sediment. Assuming that moment fixing can be expressed by an exponential function for every sediment, a half fixing depth $Z_{1/2}$ expresses a physical property of each sediment like a half life of a radio-isotope. A conception of the $Z_{1/2}$ makes a great contribution to a comprehensive understanding of different records of magnetization which appear to be complicated.

10.2 Analysis of the seven core data

Magnetization measurements of the seven core-sediments from central to south-western Japan provide three positive proofs of the present model. First, declination and inclination curves differ among cores in amlitude, although they show similar changes in shape. This is considered to be due to the effect of filtering by gradual fixing of magnetic moments. Second, there is strong correlation between directional dispersion, differential direction and observed intensity. The correlativity in the three curves shows that magnetization scatters in direction and drops in intensity where magnetization direction steeply changes along depth. This phenomenum is exactly ascribed to the magnetizing process with integration of the geomagnetic field variation. Third, remanent intensity change can be explained by the intensity reduction due to moment cancellation resulted from integration of field direction changing.

10.2.1 Deconvolution

The declination and inclination curves in Fig.15, operated with deconvolution, show that amplitude of a swing which differs among cores becomes almost equal after deconvolution. This suggests that magnetization of each core has been magnetized in the same geomagnetic field and the field can be reconstructed by the deconvolution. Major swings common in each core were extracted even from almost flat curve of remanence direction in the core HR1 and then the directional curves could be correlated with other cores'. Thus the model provides a useful technique to reconstruct the original field variation from magnetization data whose directional changes are smoothed out.

10.2.2 Internal consistency

Correlation among directional dispersion, differential direction and remanent intensity of magnetization in a sediment column can be used as an indicator of internal consistency to judge whether original remanence has been preserved without any secondary disturbance. As mentioned above, remanence acquired through the magnetizing process of the present model must have such correlation and the geomagnetic secular variation can be deduced from the remanence by deconvolution. On the other hand, the remanence without the correlation, e.g. that of the core OS1, can be regarded as a disturbed one or the one acquired through some other distinct process. Considering that the magnetization curve of OS1 does not coincide with any of other cores', it should be regarded to have been subjected to some secondary disturbance. The sediment of OS1 was semi-dried when its magnetization was measured. Hence we can easily infer that some secondary magnetization should have been overprinted during drainage of moisture, as a result that original remanence was disturbed. Sediment samples of other cores have continued to preserve the original magnetization acquired through the magnetizing process shown by the present model.

The internal consistency can be used to assess the quality of magnetization. Remanence of the core KZ3 has the normal correlation pattern, but it is very weak. It is probably because of inhomogeneity of the sediment that the correlation is not so sharp as that of OS2. Lower half of the sediment of KZ3 consists of Laminae with clay and organic material. This matter implies that half fixing depth largely changes with depth and therefore a geomagnetic field was recorded through an irregular system. Declination and inclination curves of the lower half are inconsistent with those of other cores. On the other hand, the upper half of the sediment of KZ3 is composed with homogeneous material and declination and inclination in this part is quite consistent with other cores'. Thus the diagonostics with the internal consistency is useful for a research of secular variation using magnetization of sediments.

10.2.3 Remanent intensity

We have found a new characteristic feature on remanent intensity of sediment. It is that the intensity drop is finely correlated with the intensity reduction due to cancellation of magnetic moments aligned in various directions. Some interpretations can be considered for this fact : (i) Intensity of a field decreases when its direction changes largely. (ii) Only moment cancellation is reflected in remanent intensity. (iii) Both components contribute to remanent intensity.

Only archeomagnetism at present can provide the intensity change of paleofield over the past several thousands years. Now, we try to assess the contribution of field intensity in the observed intensity of the core OS2 using the paleointensity from archeomagnetism. Fig.22 shows the paleofield intensities from archeomagnetism in Japan and Middle East (Sakai, 1980), comparing with the observed intensity curve NRM/SIRM and the calculated

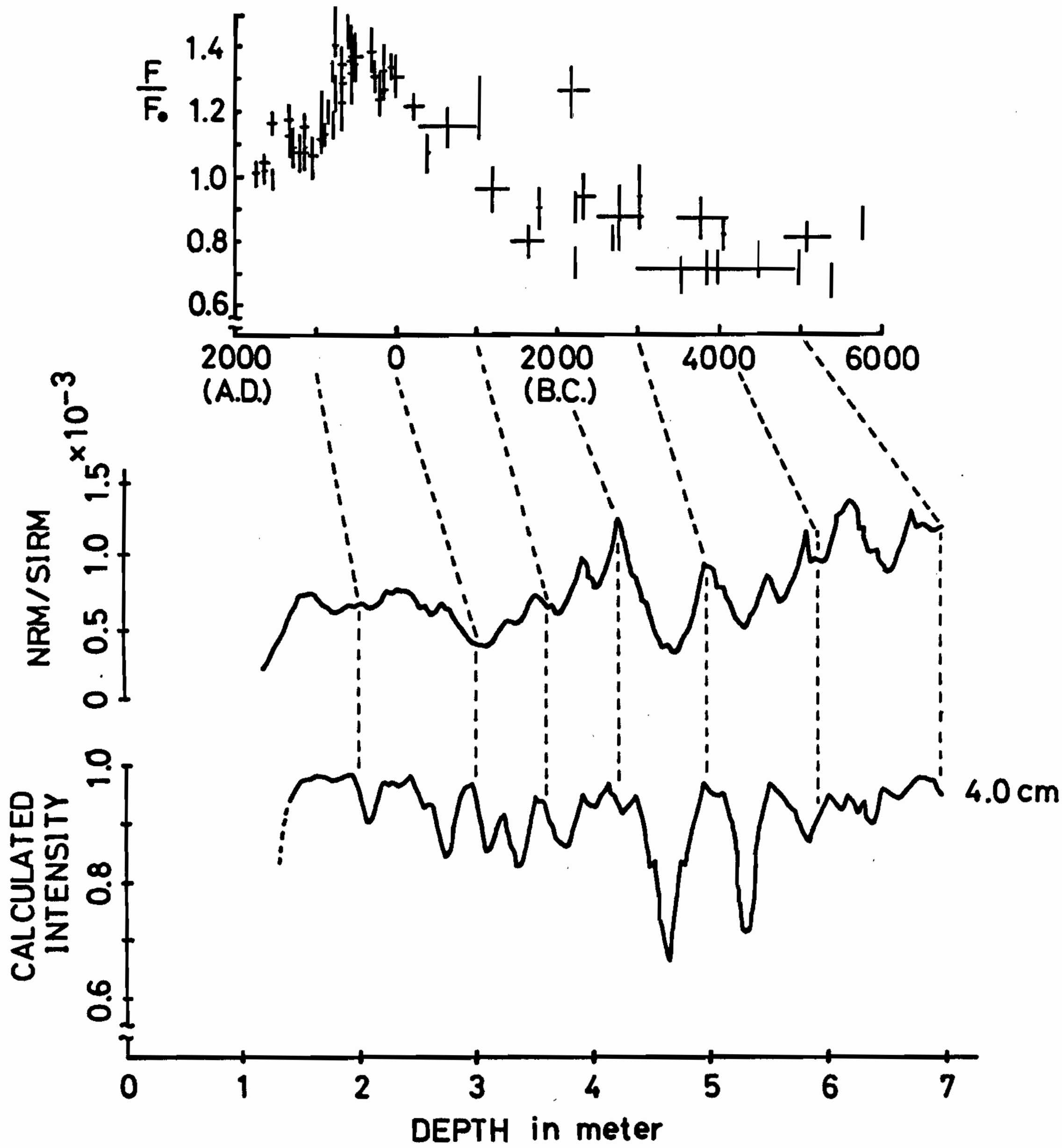

Fig.23 Comparison of three kinds of intensity changes. Variation of the geomagnetic field intensity from archeomagnetism in Japan and the Middle East (after Sakai, 1981) (top). Variation curve of NRM/SIRM intensity in the core OS2 (middle). Intensity change due to cancellation on the core OS2 calculated with $Z_{1/2}$= 4.0 cm (bottom). The broken lines show the same age horizons every 1000 years based on the age axis in Fig.20.

intensity variation due to only the cancellation effect calculated with the $Z_{1/2}$= 4.0 cm. The archeomagnetic data represent a high field period whose peak is around 500 years A.D. and a long duration of low field from 1000 years B.C. through back to 6000 years B.P.. This trend is similar to that from archeomagnetism in south-eastern Europe (Kovacheva, 1980), although they have some discrepancy in the position of the high peak. Same age harizons are linked based on the sediment ages determined in chapter 9.1. The observed intensity does not coincide with the archeomagnetic paleointensity in the position of high peak and even in trend. We can easily recognize that shape of the observed intensity curve mostly depend on the calculated intensity. In particular, the general trend of increasing with depth and the positions of small peaks and valleys bellow 4 m quite well correspond to each other. This fact suggests that the component of cancellation effect greatly contributes to the magnetization intensity and the contribution of the field intensity is quite small.

We must note that high amplitude change of the observed intensity can not still be explained completely by only the intensity decrease due to cancellation. It is likely that the cancellation gives rise to nonlinear decrease in intensity. Then some modification should be required for the present model (Hyodo, 1984). It has also been discussed that long wavelength change of the observed intensity is caused by the change in costituents of sediment, especially the change of grain size and short wavelength change is explained by the intensity decrease due to cancellation (Hyodo & Yaskawa, 1984a). Anyway, the remanent intensity of sediment does not directly reflect a field intensity and it appears to be impossible to obtain a paleointensity curve which coincides with that from archeomagnetism from the remanence of sediments even if the intensity component due to cancellation is removed.

10.2.4 Half fixing depth

The relation between the mean half fixing dpeth $\overline{Z_{1/2}}$ and mean amplitude of directional change $\overline{Am}$ agrees well with the amplitude attenuation shown by the present model in Fig.3. This fact indicates that the estimates of $Z_{1/2}$ are reasonable ones. According to the description of each core sediment in Table 1, the sediments of the cores OS3, HR1 and KZ3 consist of silty clay, silt and organic material, respectively, while those of other cores consist of fine clay. The three cores appear to be coarser grain sediments. Moreover all of them have large half fixing depths. The sediment of HR1 consisting of the coarsest grains has the largest $Z_{1/2}$. It is likely that the grain size is one of the main factors determining the $Z_{1/2}$ and the sediment of coarser grains has the larger $Z_{1/2}$.

There is some other evidence supporting the above relation between $Z_{1/2}$ and grain size. The lowest part of coarse sands in the core MZ1 has larger dispersion of direction and smaller intensity than the upper part of fine clay. This is considered to be caused by the more frequent realignments of magnetic grains (Hyodo & Yaskawa, 1984a). According to an experiment remagnetizing natural sediments in a laboratory, a sediment rich in sand shows a high possibility of remagnetizing (Payne &

Verosub, 1982). Namely, these two facts indicate that a coarse-grain sediment has a large $Z_{1/2}$.

The portion of coarse grains in the core MZ1 has a larger bulk density than that of the remaining portion with fine clay. Density of the solid grains in the core is uniform throughout the length according to the measurement (Yamamoto, 1984). This fact suggests that coaser sediment has the more closed packing, i.e. the more volume is occupied with solid materials in the coarser sediment. The core HR1 has an extremely large bulk density in comparison with those of other cores (Table 1). This may suggest that it is because of the dense structure that the sediment of HR1 composed with the coarsest grains shows the largest $Z_{1/2}$ and has the largest bulk density. It is easily expected that the dense structure in the sediment including large grains is caused by a broad distribution of grain sizes, and then magnetic grains of various sizes are locked in over the wide depth range. The distribution of grain sizes may be a dominant factor determining the $Z_{1/2}$ rather than the size of grains. However, the coarseness of sediments appears to become an indicator of the broad distribution in grain size.

The analysis of the seven core samples comes to the conclusion that the best method to obtain a secular variation from magnetization of sediments is as follows : Homogeneous fine-grained sediments which have been deposited at a uniform rate but rapidly as possible should be sampled and be measured earlier before dried.

10.3 AF-demagnetization

Remanence of a pilot specimen from the core HR1 after stepwise AF-demagnetization largely moves in direction at each step. First, it is considered that this is caused by removed soft components due to viscous remanent magnetization (VRM). However, the systematic shifting of magnetization direction after demagnetization, which sometime show even a curved line, can not be explained by them only. Another possible explanation is that each component of different coercivity has been fixed at different time, and therefore directions of individual components should align in various directions of the geomagnetic field of different ages. Stepwise AF-demagnetization gradually separates the components of different-age field. The growing-up of swings in declination and inclination curves after AF-demagnetization appears to be similar to the phenomenum by the deconvolution of magnetization data using the linear system model.

We consider fixing of magnetic grains of different coercivity in connection with the model. Two major types of fixing can be considered : (I) magnetic grains are gradually fixed in order of coercivity, and (II) fixing is independent on coercivity. The two types of the fixing can be expressed in the moment fixing function r(t) as shown in Fig.24. Time axis (t) is used here. The partition in the moment fixing function r(t) shows distribution of domains occupied by components with various coercivity. The two types of fixing can be distinguished by a result of stepwise AF-demagnetization. The magnetization by the fixing of type II will not move in direction after

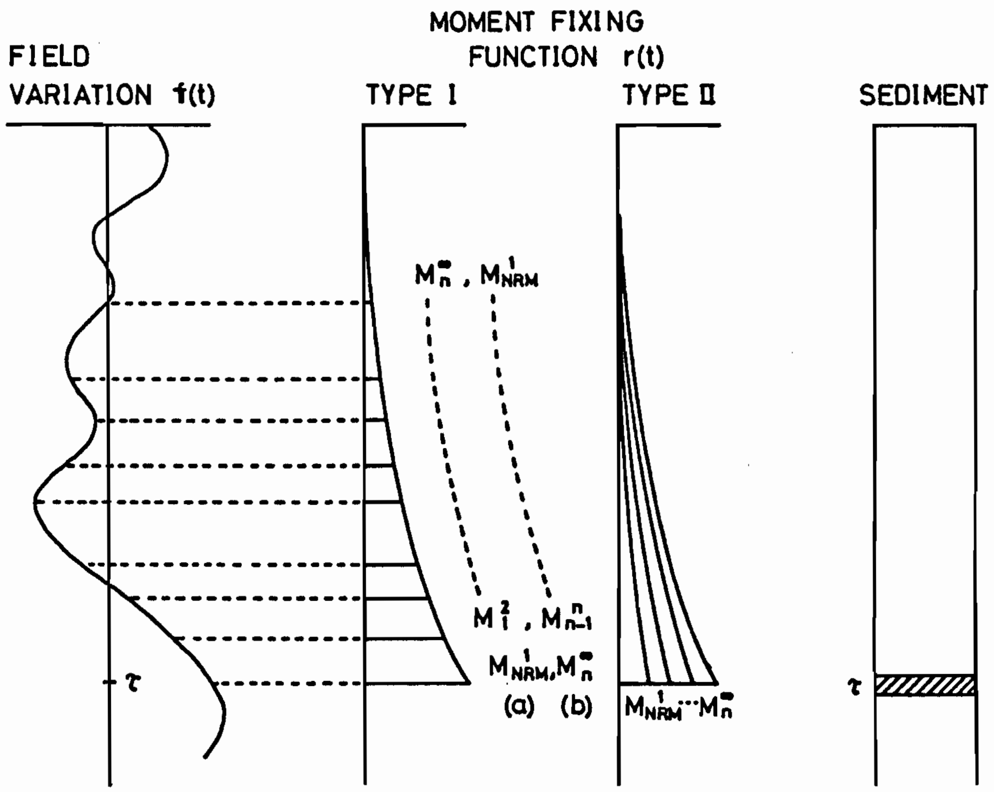

M_i^{i+1} ; Magnetization component removed by the AF-demagnetization with the i-th to (i+1)-th peak field.

Fig.24 A schematic view of the model showing that magnetization of sediment sheet of age τ is a resultant of convolution integral of a field variation f(t) and a moment fixing function r(t). Two types of moment fixing are shown in r(t). Individual magnetization components by type I fixing integrate the field variation with different time spans as shown by broken lines. All components by type II fixing integrate the same field.

AF-demagnetization, since all components integrate the same geomagnetic field with the same time span. If magnetization is acquired by the fixing of type I, each component is aligned in the different direction of a field because of the different time of fixation, and then partial demagnetization brings shifting of the remanence direction. Experimental results on the core HR1 can be exactly explained by the model of type I.

The type I fixing is further divided into two cases ; fixing begins with (a) softer components or (b) harders (Fig.24). Pilot set of specimens from the horizon HR411 at depth 517 cm, where the NRM change curve shows that declination goes eastward and inclination descends as depth goes up, show the eastward and downward shift of remanence direction after stepwise AF-demagnetization. This fact may imply the high possibility of the fixing type I(b). There is a result of an experiment by redeposition which supports the type I(b) fixing : harder components are fixed at first stage of compaction and softers at last (Payne & Verosub, 1982).

It is considered that small amplitude change in declination and inclination of the NRM is caused by the filtering effect, i.e. the directional curve of magneization is smoothed out by superposition of magnetic components aligned in the geomagnetic field direction over some time span. The operation of partial demagnetization reduces the time span of the field variation covered by remanences of individual specimens, as a result that the magnetization curve after demagnetization approaches to the field variation without amplitude attenuation. The two phenomena after AF-demagnetization, the directional parallel shifting and the growing-up of swings in directional curves, are thus explained by the model described in Fig.24. Moreover, it is demonstrated that the operation of AF-demagnetization to PDRM is equivalent to that of deconvolution.

10.4 Secular variation

Secular variation of the geomagnetic field is generally explained by moving non-dipole sources. The analysis of the worldwide field elements during the last several hundreds years reveals that the non-dipole source has been drifting westward about 0.2° per year (Bullard et al., 1950 ; Yukutake & Tachinaka, 1968). Such drifting of a magnetic source can be observed in a local field at a single site on the earth's surface, for the drifting causes a looping motion in the field direction, clockwise or counterclockwise. Furthermore there is a rule that a clockwise looping of the field direction viewed toward its north-seeking end is caused by the westward drifting of the magnetic source and a counter-clockwise looping by the eastward drifting (Runcorn, 1959). This is recognized by numerical calculations with radial dipole sources (Skiles, 1970). Based on the rule, the motion of a non-dipole source can be inferred in the past beyond the limit that observatory data are obtainable, using paleomagnetic data.

The motion of the paleomagnetic field direction for the last 7000 years recorded in the core OS2 is represented on an equal area map in Fig.25. The field direction continuouly loops three times clockwise during the period from about 7000 to 5500 years

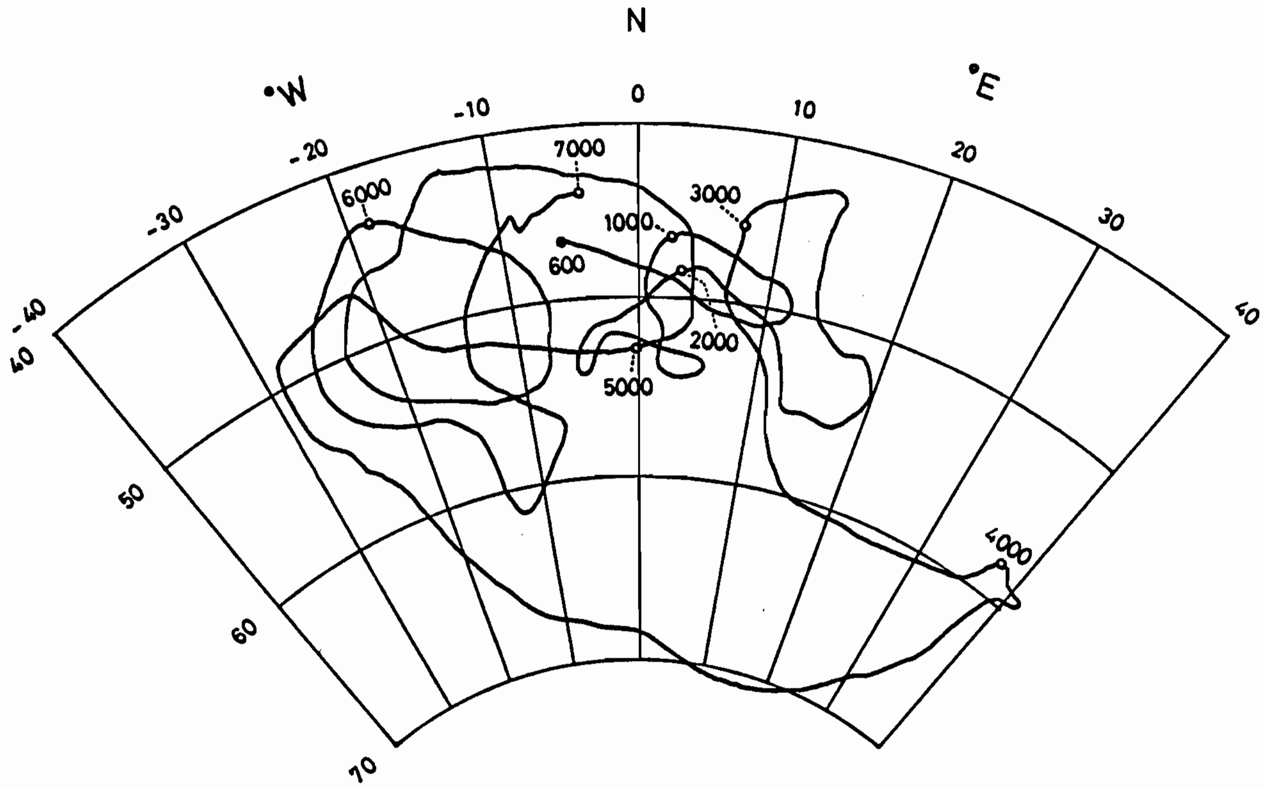

Fig.25 An equal area stereographic projection of the secular variation of the geomagnetic field direction in central to south-western Japan for the last 7000 years.

B.P. Each loop has almost the same period, about 500 years. After moved along a half large loop counterclockwise from 5500 to 4500 years B.P., the clockwise and counterclockwise loops are alternatively repeated. Their periods are about 500 to 1000 years. The prevailing period of the looping for the last 7000 years appears to be less than 1000 years, departing from the period of 1800 years calculated with the drifting rate 0.2 /yr of the present non-dipole source. Except the tripple clockwise loops from 7000 to 5500 years B.P., there is no evidence that the westward drift shown by the present non-dipole source has been prevailing for the last several thousand years. It is thus revealed that the present motion of the magnetic source on the surface of the earth' core has not persisted beyond several hundreds years ago. This places substantial constraints on the modeling of the earth's field dynamo as the magnetic reversal at once brought the two-disc dynamo (Rikitake, 1958).

11. Conclusion

The introduction of the linear system model for the magnetizing process in sediments allows the various features of DRM to be explained comprehensively. For example, the correlativity among the change curves of directional dispersion, differential direction and remanent intensity is a resultant effect of the field integration. In addition, the average amplitude of directional changes of remanence is a function of the average half fixing depth as expected by the model.

A main factor determining the width of magnetizing zone is the size distribution of sediment grains. The coarse grained sediments possess the broad distribution of grain size and they have large half fixing depth. On the other hand, fine clay can be a good recorder of the geomagnetic field with small effect of filtering due to the narrow zone of magnetizing. Moreover, homogeneity of the size distribution throughout length is an important factor as the good recorder.

The deconvolution is an useful method to deduce the geomagnetic secular variation from remanence of sediments, especially from the one whose half fixing depth is quite large. The operation of AF-demagnetization is equivalent to that of deconvolution. It would become a powerful technique to reconstruct the geomagnetic secular variation from the remanence whose directional changes are smoothed out, along with the deconvolution method.

A secular variation curve of the field direction from the remanence of sediments coincides with that from archeomagnetism for the last 2000 years. However, the change of remanent intensity quite differs with the archeomagnetic paleointensity. The intensity curve is rather reflected by the intensity reduction due to cancellation of magnetic moments resulted from the integration of field variation.

The secular variation in central to south-western Japan for the last 7000 years shows evidence of both westward and eastward driftings of non-dipole sources. The two driftings equally occur at least for the last 3000 years. The present motion of the westward drifting would be a temporary one.

The new techniques proposed in the present study, the deconvolution and the method to assess the quality of magnetization records, enhance the reliability of the secular variation from remanence of sediments. Paleomagnetic study using these techniques would greatly contribute to the development of geomagnetism.

REFERENCES

Arai, H., Personal communication, 1981.

Barton, C.E. and M.W. McElhiny, Detrital remanent magnetization in five slowly redeposited long cores of sediment, Geophys. Res. Lett., 6, 229-232, 1979.

Bullard, E.C., C. Freedman, H. Gellman and J. Nixon, The westward drift of the earth's magnetic field, Phil. Trans. Roy. Soc. London, A, 243, 67-92, 1950.

Clark, H.C., and J.P. Kennet, Paleomagnetic excursion recorded in latest pleistocene deep-sea sediments, Gulf of Mexico, Earth planet. Sci. Lett., 19, 267-274, 1973.

Creer, K.M., R. Thompson, L. Molyneux and F.J.H. Mackereth, Geomagnetic secular variation recorded in the stable magnetic remanence of recent sediments, Earth planet. Sci. Lett., 14, 115-127, 1972.

Creer, K.M., D.L. Gross, and J.A. Lineback, Origin of regional geomagnetic variations recorded by Wisconsin and Holocene sediments from Lake Michigan, U.S.A. and Lake Windermere, England, Geol. Soc. Amer. Bull., 87, 531-540, 1976.

Cox, A., R.R. Doell and G.B. Dalrymple, Geomagnetic polarity epocks and pleistocene geochronometry, Nature, 198, 1049-1051, 1963.

Cox, A., R.R. Doell and G.B. Dalrymple, Reversals of the earth's magnetic field, Science, 144, 1537-1543, 1964.

Denham, C.R., Counter-clockwise motion of paleomagnetic directions 24000 years ago at Mono lake, California, J. Geomag. Geoelectr., 26, 487-498, 1974.

Hamano, Y., An experiment on the post-depositional remanent magnetization in artificial and natural sediments, Earth planet. Sci. Lett., 51, 221-232, 1980.

Harrison, C.G.A. and B.L.K. Somayajulu, Behavior of the earth's magnetic field during a reversal, Nature, 212, 1193-1195, 1966.

Hirooka, K., Archeomagnetic study for the past 2000 years in southwest Japan, Mem. Fac. Sci. Kyoto Univ., 38, 167-207, 1971.

Horie, S., K. Yaskawa, A. Yamamoto, T. Yokoyama and M. Hyodo, Paleolimnology of Lake Kizaki, Arch. Hydrobiol., 89, 407-415, 1980.

Hyodo, M. and K. Yaskawa, Geomagnetic secular variation recorded in the stable magnetic remanence of the young sediments collected from Osaka Bay, J. Geomag. Geoelectr., 32, 581-584, 1980.

Hyodo, M., S. Onishi and K. Yaskawa, Internal consistency of paleomagnetic records in sediments, Rock Mag. Paleogeophys., 10, 29-32, 1983.

Hyodo, M., Possibility of reconstruction of the past geomagnetic field from homogeneous sediments, J. Geomag. Geoelectr., 36, 45-62, 1984.

Hyodo, M., H. Morinaga, H. Nishimura H. Inokuchi and K. Yaskawa, Paleomagnetism of a core from Osaka Bay II, submitted to J. Geomag. Geoelectr., 1984.

Hyodo, M. and K. Yaskawa, Paleomagnetism of a core-sediment from the Inland Sea, Japan (Seto Naikai) I, submitted to Geophys. J. R. astro. Soc., 1984a.

Hyodo, M. and K. Yaskawa, Paleomagnetism of a core from the Inland Sea, Japan (Seto Naikai) II : a secular variation recorded in coarse-grained sediments, submitted to J. Geomag. Geoeletcr., 1984b.

Hyodo, M. and K. Yaskawa, Paleomagnetism of a core from Lake Yogo, to be submitted to J. Geomag. Geoelectr., 1984c.

Irving, E., The origin of the paleomagnetism of the Torridonian Sandstone series of northwest Scotland, Phil. Trans. Roy. Soc. Lond. A, 250, 100-110, 1957.

Irving, E. and A. Major, Post-depositional detrital remanent magnetization in a synthetic sediment, Sedimentology, 3, 135-143, 1964.

Kent, D. V., Post-depositional remanent magnetization in deep-sea sediment, Nature, 246, 32-34, 1973.

Kobayashi, K., K. Kitazawa, T. Kanaya and T. Sakai, Magnetic and micropaleontological study of deep-sea sediments from the west central Pacific, Deep-Sea Res., 18, 1045-1062, 1971.

Kovacheva, M., Summarized results of the archeomagnetic investigation of the geomagnetic field variation for the last 8000 yr in south-western Europe, Geophys. J. R. astr. Soc., 61, 57-64, 1980.

LaBrecque, J.L., D.V. Kent and S.C. Cande, Revised magnetic polarity time scale for late Cretaceous and Cenozoic time, Geology, 5, 330-335, 1977.

Løvlie, R., Post-depositional remanent magnetization in a re-deposited deep-sea sediment, Earth. planet. Sci. Lett., 21, 315-321, 1974.

Løvlie, R., The intensity pattern of post-depositional remanence acquired in some marine sediments deposited during a reversal of the external magnetic field, Earth planet. Sci. Lett., 30, 209-214, 1976.

Lund, S.P., D. Bogdan, S. Levi, S.K. Banerjee and A. Long, Continuous geomagnetic record for the past 10,000 years from Lake St. Croix, Minnesota, EOS (Trans. Amer. Geophys. Un.), 57, 910, 1976.

Mackereth, F.H., On the variation in direction of the horizontal component of remanent magnetization in lake sediments, Earth planet. Sci. Lett., 12, 332-338, 1971.

Matsuda, J., M. Hyodo, H. Inokuchi, N. Isezaki and K. Yaskawa, A new alternating field demagnetizer for paleomagnetic studies without rotation of specimen, J. Geomag. Geoelectr., 33, 161-170, 1981.

Muroi, I. and K. Yaskawa, Paleomagnetism of Osaka Bay sediments, Rock Mag. Paleogeophys., 4, 76-80, 1977.

Niitsuma, N., Zone-magnetization model and depth lag of NRM in deep-sea sediments, Rock Magn. Paleogeophys., 4, 65-71, 1977.

Opdyke, N.D., B. Glass, D. Hays and J.H. Foster, Paleomagnetic study of Antarctic deep-sea cores, Science, 154, 349-357, 1966.

Otofuji, Y. and S. Sasajima, A magnetization process of sediments : laboratory experiments on post-depositional remanent magnetization, Geophys. J. R. astr. Soc., 66, 241-259, 1981.

Payne, M. A. and Verosub K. L., The acquisition of post-depositional detrital remanent magnetization in a variety of natural sediments, Geophys. J. R. astro. Soc., 63, 625-642, 1982.

Rikitake, T., Oscillations of a system of disk dynamo, Proc. Cambridge Phil. Soc., 54, 89-105, 1958.

Runcorn, S.K., On the theory of the geomagnetic secular, variation, Ann. de Geophys., 15, 87-92, 1959.

Sato, T., Paleomagnetic field intensity obtained by use of deep-sea cores of Quaternary, PhD Thesis, Osaka Univ., Osaka, Japan, 1980.

Sakai, H., Variation of the geomagnetic field intensity deduced from archeological objects, Rock Magn. Paleogeophys., 7, 61-67, 1980.

Skiles, D.D., A method of inffering the direction of drift of the geomagnetic field from paleomagnetic data, J. Geomag. Geoelectr., 22, 441-462, 1970.

Tucker, P., A grain mobility model of post-depositional realignment, Geophys. J. R. astr. Soc., 63, 149-163, 1980.

Turner, G. M. and R. Thompson, Lake sediment record of the geomagnetic secular variation in Britain during Holocene times, Geophys. J. R. astr. Soc., 65, 703-725, 1981.

Yamamoto, A., Personal communication, 1984.

Yaskawa, K., When did magnetization fix in loose sediment ?, Rock Magn. Paleogeophys., 2, 15-19, 1974.

Yaskawa, K., T. Nakajima, M. Torii and N. Kawai, Paleomagnetism of a core from Lake Biwa (I), J. Geomag. Geoelectr., 25, 447-474, 1973.

Yukutake, T. and H. Tachinaka, The westward drift of the geomagnetic secular variation, Bull. Earthq. Res. Inst., 46, 1075-1102, 1968.